Impact of land use on the hydraulic properties of the topsoil in a small French catchment

E. Gonzalez Sosa, I. Braud, J. Dehotin, L. Lassabatère, R. Angulo Jaramillo, M. Lagouy, F. Branger, C. Jacqueminet, S. Kermadi, K. Michell

Author-produced version of the article published in Hydrological Processes, vol. 24, n° 17
The original publication is available at http://www3.interscience.wiley.com doi : 10.1002/hyp.7640

Impact of land use on the hydraulic properties of the topsoil in a small French catchment

E. Gonzalez-Sosa,[1,2] I. Braud, [1*] J. Dehotin,[1] L. Lassabatère,[3] R. Angulo-Jaramillo,[4, 5] M. Lagouy[1], F. Branger[1], C. Jacqueminet[6], S. Kermadi[6], K. Michell[6]

[1] Cemagref, UR HHLY, CP 220, 3bis Quai Chauveau, 69336 Lyon Cédex 9, France

[2] DEFI-CIAQ, Université de Querétaro, CU Cerro de las Campanas. S/N. Centro. 6900 Queretaro, Qro., Mexico

[3] Laboratoire Central des Ponts et Chaussées, Division Eau et Environnement, Route de Bouaye, 44381 Bouguenais Cedex, France.

[4]Université de Lyon, ENTPE, rue Maurice Audin, 69518 Vaulx-en-Velin, France

[5] LTHE, CNRS, BP 53, 38041 Grenoble Cedex 9, France

[6]Université de Lyon, UMR CNRS EVS, 18 rue de Chevreul, F-69 364 Lyon Cedex, France

* Correspondance to: Isabelle Braud, Cemagref, UR HHLY, CP 220, 3bis Quai Chauveau, 69336 Lyon cedex 9, France

E-mail : Isabelle.Braud@cemagref.fr

Hydrological Processes, 2010, Vol 24, 2382-2399, DOI: 10.10002/hyp.7640

Abstract

The hydraulic properties of the topsoil control the partition of rainfall into infiltration and runoff at the soil surface. They must be characterized for distributed hydrological modelling. This study presents the results of a field campaign documenting topsoil hydraulic properties in a small French suburban catchment (7 km^2) located near Lyon, France. Two types of infiltration tests were performed: single ring infiltration tests under positive head and tension disk infiltration using a mini-disk. Both categories were processed using the BEST –*Beerkan* Estimation of Soil Transfer parameters- method to derive parameters describing the retention and hydraulic conductivity curves. Dry bulk density and particle size data were also sampled. Almost all the topsoils were found to belong to the sandy loam soil class. No significant differences in hydraulic properties were found in terms of pedologic units, but the results showed a high impact of land use on these properties. The lowest dry bulk density values were obtained in forested soils with the highest organic matter content. Permanent pasture soils showed intermediate values, whereas the highest values were encountered in cultivated lands. For saturated hydraulic conductivity, the highest values were found in broad leaved forests and small woods. The complementary use of tension disk and positive head infiltration tests highlighted a sharp increase of hydraulic conductivity between near saturation and saturated conditions, attributed to macroporosity effect. The ratio of median saturated hydraulic conductivity to median hydraulic conductivity at a pressure of -20 mm of water, was about 50. The study suggests that soil texture, such as used in most pedo-transfer functions, might not be sufficient to properly map the variability of soil hydraulic properties. Land use information should be considered in the parameterizations of topsoil within hydrological models to better represent *in situ* conditions, as illustrated in the paper.

Author-produced version of the article published in Hydrological Processes, vol. 24, n° 17
The original publication is available at http://www3.interscience.wiley.com doi : 10.1002/hyp.7640

Keywords: soil hydraulic properties, infiltration tests, BEST method, land use impact, hydraulic properties mapping

INTRODUCTION AND CONTEXT

Soil surface thermal and hydraulic properties control heat and water exchange at the soil vegetation atmosphere interface through their impact on infiltration and the surface energy balance. Therefore, they play a central role in the correct understanding and modelling of water balance, surface processes, evapotranspiration, groundwater recharge, erosion or pollutant transport. Human activities such as agricultural practices (ploughing, sowing), changes in land use related to urbanisation, industrial activity, deforestation or reforestation of abandoned agricultural land can significantly affect topsoil and first layers hydraulic properties. The accurate representation of soil hydraulic properties within hydrological models is therefore necessary to reliably represent the water balance and hydrological responses. In many hydrological models, soil hydraulic properties are determined based on pedo-transfer functions. These functions relate easily accessible soil properties such as soil texture (e.g. Clapp and Hornberger, 1978; Cosby *et al.*, 1984) or soil texture, organic matter content and dry bulk density (e.g. Rawls and Brackensiek, 1985; Verecken *et al.*, 1989; Wösten, 1997) to soil hydraulic properties (retention and hydraulic conductivity curves). Existing pedo-transfer functions have been in general calibrated on limited soil samples and are often region specific. As an illustration, the pedotranfer functions of Cosby *et al.*, (1984) and Rawls and Brackensiek (1985) were calibrated on US soils. Verecken *et al.* (1989) used soil samples from Belgium, and Wösten (1997) the HYPRES European soil data base (Wösten *et al.*, 1999). Different conclusions have been reached about the use of pedotransfer functions in hydrological models. Some studies have concluded that existing pedo-transfer functions are adequate (e.g. Islam *et al.*, 2006) whereas other authors question their usefulness for a correct assessment of hydrological water balances (e.g. Sobieraj *et al.*, 2001; Gutman and Small, 2005). Wösten *et al.* (2001) underline the usefulness of pedotransfer functions but

Author-produced version of the article published in Hydrological Processes, vol. 24, n° 17
The original publication is available at http://www3.interscience.wiley.com doi : 10.1002/hyp.7640

discourage their use for soils that are outside their range of applications, while calling for the collection of large data sets to document soil hydraulic properties worldwide.

The present study is based on these recommendations and contributes to the documentation of soil hydraulic properties in a small French suburban catchment. Suburban catchments generally experience a large and quick land-use change, such as an increase of impervious areas, but also sometimes, desertion of farming lands that turn into fallow lands, and finally into sporadic deciduous forests. Rivers and runoff are also affected through straightening of natural water courses and runoff concentration into pipes for instance. A higher proportion of built infrastructures has a significant impact on hydrologic and ecosystem functions and often result in excess runoff, lower groundwater recharge and pollution (e.g., Bras and Perkins, 1975; Desbordes, 1989; Chocat *et al.*, 2001; Booth *et al.*, 2002; Randhir, 2003; Matteo *et al.*, 2006; Marsalek *et al.*, 2007). The vulnerability of these areas to floods, droughts and water quality problems is therefore increased.

The Yzeron catchment (150 km^2) is located to the south-west of Lyon city (Figure 1). This catchment is representative of many suburban catchments. Since the fifties, it has experienced rapid changes of land use, due to the vicinity of Lyon city. Two different trends can be observed since the middle of the 20th century. The first one is an increase of the catchment urbanisation, with a full urbanised area in the downstream part. The second trend is a decrease of cultivated land explained by the urbanisation, but also by an increase of the forested areas in relation with the decline of agricultural activities (Gnouma, 2006). In recent years, several problems have been identified: an increase in the frequency of flooding (Radojevic, 2002), increased pollution problems (Lafont *et al*., 2006), and increased erosion of the river banks associated with adverse effects on water quality (Schmitt *et al.*, 2008). The water responsible for these flooding events comes mainly from the rural part of the catchment, but its effect can be enhanced by fast contributions from urbanised zones having short runoff lag time

Author-produced version of the article published in Hydrological Processes, vol. 24, n° 17
The original publication is available at http://www3.interscience.wiley.com doi : 10.1002/hyp.7640

(Radojevic, 2002). These disorders must be reduced to comply with the requirements of the water framework directive. It is therefore important to better quantify the impact of land use changes on the hydrological regime of this catchment. For this purpose, a distributed hydrological model of the catchment is being developed, that takes into account both the rural and the urbanised areas. Given the importance of rural areas on the Yzeron regime, it was necessary to acquire improved knowledge on the soil hydraulic properties within the catchment and propose rules for their specification in the elementary meshes of the distributed hydrological model (from a few hectares to a few km^2). This task is of course challenging, because it is not possible to measure soil hydraulic properties everywhere and we wanted to propose alternative solutions to the use of pedo-transfer functions only, by introducing *in situ* observations in the mapping process.

The objectives of the study were the following: (i) to document the spatial variability of soil hydraulic properties (including both the retention and hydraulic conductivity curves) within the catchment using relevant *in situ* measurements and an adequate sampling strategy; (ii) to analyse the links between the spatial variability of hydraulic properties and pedology and land use; (iii) to use these measurements to derive rules for the mapping of soil hydraulic properties as required in distributed hydrological modelling.

MATERIALS AND METHODS

Catchment description

The Yzeron catchment is located south-west of Lyon city in the “Mont du Lyonnais” area (Figure 1). The topography ranges from a maximum of 917 m above sea level in the western part to a minimum of 162 m at the outlet. The highest slopes are encountered in the western part of the catchment and along the river network and the lowest slopes are located in the eastern part (Figure 1). The geology is composed mainly of gneiss and granite. The average annual rainfall is 800 mm and the average annual minimum and maximum temperatures are 6.8 °C and 15.8 °C, respectively (Gnouma, 2006). The catchment forms part of a long term observatory called Observatoire de Terrain en Hydrologie Urbaine (OTHU, 2010), dedicated to the study of the impact of urbanisation on hydrology. In this framework, two sub-catchments have been monitored since 1997. The first one, the Mercier catchment (7 km^2) is considered as a natural catchment and is covered mainly with forests and crops. The second one, the Chaudanne catchment (2.5 km^2) is mainly covered with crops and urbanised areas (Figure 1). The Mercier catchment shows a large spatial variability of soils, with the presence of 8 soil pedological units over a total of 22 present within the whole Yzeron catchment, according to the Sol Info Rhône Alpes pedology map (SIRA, 2010). The Mercier catchment soils are also representative of the rural area of the Chaudanne catchment. The study presented here is therefore focused on the Mercier catchment. In this basin, the elevation ranges from 400 m and 800 m with a marked topography and slopes commonly higher than 10%. The land use is dominated by forest, pasture and crops, although a significant part of the catchment is affected by human activity with the existence of small villages and a quite dense road network.

Sampling strategy

The sites were selected to include the maximum combinations of factors that can influence soil hydraulic properties such as pedology and land use. For this purpose, we used the pedology map, provided by Sol Info Rhône Alpes at scale 1/250000 (Figure 2, SIRA, 2010) and the 2000 Corine Land Cover map provided by the Service de l'Observation et des Statistiques (SOeS, 2010). The distribution from the land use map showed that the forest area (mountain) represents about 33%, pasture 32% and complex cultivation pattern accounts for about 30% of the total basin area. Urbanised surface is less than 6% of the total surface. Regarding soil classes, soil 102 (loamy sand and clayey sand – see Table I**)** covers more than 50% of the basin area. From this analysis, nine soil classes and six land uses from the Corine map were retained that accounted for most of the total area and a first selection of sites was performed in order to sample the maximum of land use/pedology combinations (17 over a total of 38 covering 90% of the catchment surface). Sites accessibility was also taken into account in the final selection. A field survey refined the selection and the land use description, especially for crops where the Corine land cover map was not detailed. Finally 20 locations were retained and sampled (Figure 2). Their distribution in terms of pedology (Soil Cartographic Units –SCU-) and land use, as retrieved from the field, is shown in Table I.

The measured points within the sites were located at least 10 m from the fields edges. With regard to topography, most of the sites were located on slopes, very few in flat zones. At the 20 locations, samples were collected in order to characterize the soil texture and the dry bulk density. Infiltration tests using single ring and mini-disk infiltrometers were performed. The field survey was restricted to the topsoil layer. The location of each infiltration test was measured using a GPS (3 m in *x* and y). The experimental protocols are described below.

Soil texture and dry bulk density measurements

Twenty-eight topsoil samples of 250-300 g were collected using augers and were analised to derive the soil particle size distribution function. Five classes were considered (clay, fine silt, coarse silt, fine sand, coarse sand) corresponding to the following fractions (<2, 2-20, 20-50, 50-200, 200-2000 µm) and were determined according to the French standard (NF X 31-107 norm), which involves sieving for the fractions >50 µm and sedimentation below 50 µm. Organic matter content was also determined using the NF ISO 10694 standard. All the analyses were done at the INRA soil laboratory in Arras .

To characterize the topsoil *A* horizon, the dry bulk density was measured using samples collected in the 0-2.5 cm depth and 0-5 cm depth layers. These samples were collected following the ISO NF X31-501 standard. The dry bulk density, ρ_d, allows the derivation of porosity once assumed a certain value for the particle density, ρ_s. In this study we used the commonly used value of $\rho_s = 2650$ kg m^{-3}and the porosity, ε, was calculated as:

$$\varepsilon = 1 - \rho_d / \rho_s \qquad (1)$$

Infiltration tests

The field campaign was conducted from October 6 to October 10 2008 by a team of five persons. At each of the twenty selected locations, infiltration tests were performed using two techniques: Mini Disk Infiltrometer (MDI) (in general two replicates per location) and single ring (SR) or *Beerkan* method (Braud *et al.*, 2005) (three replicates per location). Their distribution with respect to pedological cartographic units and land uses is shown in Table I.

Braud *et al.* (2005) proposed an experimental protocol for the single ring infiltration tests, with cylinders of 5-15 cm in diameter. According to this protocol, about 8-15 equal volumes of water must be poured successively into the cylinders. The infiltration times of these water volumes are measured. In our study, the cylinders used for the SR tests were 400 mm in diameter and 225 mm in height. They were much larger than recommended by Braud *et al.* (2005). The reason of this choice is the wish to average the soil spatial heterogeneity by sampling a larger surface, in order to obtain measures representative of the fields. As a consequence, the infiltration protocol had to be modified as compared to Braud *et al.* (2005). Before each SR test, the litter and vegetation leaves were removed, as in Bodhinayake and Si (2004). If necessary, the vegetation was cut but roots were left in place. The cylinders were inserted 2-5 cm deep into the soil, in order to ensure water tightness and avoid leaks, without perturbing too much the 3-D water flow. In all cases 12 L of fresh (15-18 °C) water were

Author-produced version of the article published in Hydrological Processes, vol. 24, n° 17
The original publication is available at http://www3.interscience.wiley.com doi : 10.1002/hyp.7640

poured within a plastic sheet, sealed to the cylinder, to minimize the disturbances in topsoil that frequently occur when water is added directly. The plastic sheet was then removed and the chronometer was started. The initial height was measured using a ruler. Then the infiltration height as a function of elapsed time was followed by reading the ruler. During the first minutes, small time intervals of a few seconds were used and the time interval was increased after 3 or 5 minutes (Herman *et al*. 2003). The operation was terminated when all the water had infiltrated the soil. Two soil samples were also collected for measurement of the initial and final gravimetric water contents (g water per g solids). For the final water content sampling, small cylinders of 43 mm in diameter and 28 mm in height were used. These samples enable us to obtain additional measurements of the dry bulk density.

For the MDI infiltration tests, we used the tension Mini-disk Infiltrometer of 135 ml in volume water capacity and 22.5 mm in radius (Decagon Devices Inc., Pullman, WA). The detritus and dead leaves were also removed before the tests started. A small layer of soil (Horizon O < 5 cm) of less than 2 cm was also removed. It was required in order to carry out the tests on horizontal surfaces and ensure the stability of the apparatus and a good contact between the infiltrometer membrane and the soil. For this we used a thin layer (< 1mm) of fine sand. The surface pressure was set to -20 mm for all the MDI infiltration tests.

Derivation of retention and hydraulic conductivity curves parameters using the BEST method

The infiltration tests were used to determine the retention curve $h(\theta)$, relating the soil water pressure h (m) to the soil volumetric water content θ (m^3 m^{-3}) and the hydraulic conductivity curve $K(\theta)$ relating the soil hydraulic conductivity K (m s^{-1}) to the soil water content. The retention curve was modeled using the van Genuchten (1980) approach:

Author-produced version of the article published in Hydrological Processes, vol. 24, n° 17
The original publication is available at http://www3.interscience.wiley.com doi : 10.1002/hyp.7640

$$\frac{\theta}{\theta_s} = \left\{1 + \left(\frac{h}{h_{VG}}\right)^n\right\}^{-m} \quad (2)$$

with $$n = \frac{k}{1-m} \quad (3)$$

where θ_s is the saturated water content (m^3 m^{-3}), h_{VG} (m) is a normalization parameter for the water pressure, *m* and *n* are shape parameters (-) and *k* is an integer which can be chosen to be 1 (Mualem, 1976) or 2 (Burdine, 1953). A value of k=2 was used in the following. A value of k=1 could have been used either as Haverkamp *et al.* (2005) provide relationships between the various formulations. Eq. (2) assumes that the residual water content at large pressure is zero.

The hydraulic conductivity curve was modeled using the Brooks and Corey (1964) model:

$$K(\theta) = K_s\left(\frac{\theta}{\theta_s}\right)^{\eta} \quad (4)$$

where K_s (m s^{-1}) is the saturated hydraulic conductivity and η is a shape parameter (-) related to *m* and *n* by:

$$\eta = \frac{2}{mn} + 2 + p \quad (5)$$

where *p* is a tortuosity parameter equal to 0 (Childs and Collis-George, 1950), 0.5 (Mualem, 1976) or 1 for the Burdine (1953) model. A value of 1 was used in this study to be consistent with the choice of the Burdine (1953) model for the retention curve in Eq. (3).

At each location, the values of the parameters of the retention and hydraulic conductivity curves as described by Eqs. (2) and (4), namely the shape parameters *m*, *n* and η and the structure parameters θ_s, h_{VG} and K_s were calculated. It was done using the BEST (*Beerkan* Estimation of Soil Transfer parameters) method proposed by Lassabatère *et al.* (2006). The first step of the BEST method corresponds to the estimation of the shape parameters *m*, *n* and

η from the soil particle size distribution data. Details can be found in Lassabatère *et al.* (2006) and are not reported here.

The second step is the optimisation of the infiltration tests in order to derive the structural parameters θ_s, h_{VG} and K_s. In this study, the saturated water content, θ_s, was determined from field final water content and dry bulk density and therefore only h_{VG} and K_s were derived from the optimisation of the infiltration tests. Two equations were used for this purpose.

For short to medium time steps, the BEST method uses an analytical approximation of the full 3D infiltration, $I_{3D}(t)$ (m), equation proposed by Haverkamp *et al.* (1994) for the interpretation of infiltration tests:

$$I_{3D}(t) = S\sqrt{t} + \left[\frac{\phi S^2}{R(\theta_0 - \theta_i)} + K_i + \frac{2-\beta}{3}(K_0 - K_i)\right]t \qquad (6)$$

where S is the sorptivity (m s$^{-1/2}$); R is the radius of the infiltrometer (m), θ_i is the initial water content and θ_0 is the final water content, K_i is the initial hydraulic conductivity (m s^{-1}) and K_0 (m s^{-1}) is the final one. $K_0 = K(h_0)$, where h_0 (m) is the water pressure at the soil surface (positive for single ring infiltration tests and negative for mini-disk infiltration tests). For the parameters β and ϕ, we used the value of ϕ=0.75 and β=0.6, shown to apply for most soils when θ_i < 0.25 θ_s (Smettem *et al.*, 1994; Haverkamp *et al.*, 1994). The sorptivity $S(\theta_i, \theta_0)$ is a function of initial and final water content but notation $S = S(\theta_i, \theta_0)$ will be used for the sake of simplicity.

The approximation provided by Eq.(6) is valid only for times t_i lower than a maximum value given in Lassabatère *et al.* (2006):

$$t_{max} = \frac{1}{4(1-B)^2} t_{grav} \qquad (7)$$

where $B = \frac{K_i}{K_0} + \frac{2-\beta}{3}\left(1 - \frac{K_i}{K_0}\right) = \left(\frac{\theta_i}{\theta_0}\right)^\eta + \frac{2-\beta}{3}\left(1 - \left(\frac{\theta_i}{\theta_0}\right)^\eta\right)$ (8)

and $$t_{grav} = \left(\frac{S}{K_0}\right)^2 \tag{9}$$

t_{grav} is the gravity time which corresponds to the time at which gravity begins to dominate the flow process (Philip, 1969).

For long time steps, Haverkamp *et al.* (1994) showed that the asymptotic infiltration can be written (subscript $_{3D}$ is omitted in the following for simplicity):

$$I_\infty = \left[K_0 + \frac{\phi S^2}{R(\theta_0 - \theta_i)}\right]t + \frac{S^2}{2(K_0 - K_i)(1-\beta)}\ln\left(\frac{1}{\beta}\right) \tag{10}$$

which corresponds to a linear variation with time. For long time steps, the infiltration flux is a constant given by the slope of the curve *I(t)* as defined by Eq. (10):

$$q_\infty = K_0 + \frac{\phi S^2}{R(\theta_0 - \theta_i)} = K_0 + AS^2 \tag{11}$$

with $$A = \frac{\phi}{R(\theta_0 - \theta_i)} \tag{12}$$

Data for large time steps are used to fit Eq. (10) using a simple regression analysis and derive the q_∞ estimate. For short times steps, we used the method proposed by Lassabatère *et al.* (2006) to optimize the sorptivity. The reader can refer to this paper for more details.

Note that, up to this step, the method can be applied both for infiltration test under suction or with a positive pressure head. Therefore it can be used for the interpretation of both the mini-disk and single ring infiltration tests.

On the other hand, the estimation of the normalization parameter h_{VG} can only be performed from the SR infiltration (Braud *et al.*, 2005) using:

$$h_{VG} = -\frac{S^2}{c_{p\_VG}(\theta_s - \theta_i)K_s\left[1 - \left(\frac{\theta_i}{\theta_s}\right)^\eta\right]} \tag{13}$$

where c_{p_VG} is a texture dependent factor, the expression of which is given by Haverkamp *et al.* (1998):

$$c_{\mathrm{p\_VG}} = \Gamma\left(1+\frac{1}{n}\right)\left\{\frac{\Gamma\left(m\eta-\frac{1}{n}\right)}{\Gamma(m\eta)}+\frac{\Gamma\left(m\eta+m-\frac{1}{n}\right)}{\Gamma(m\eta+m)}\right\} \tag{14}$$

where Γ is the classical incomplete Gamma function.

Up to now, only positive head infiltration tests have been analysed using the BEST method (de Souza *et al*., 2008; Mubarak *et al*., 2009; Xu *et al*., 2009). The only exception is the case study by Scalenghe and Ferraris (2009) that also analysed tension-disk infiltration tests with the method. To our knowledge, it is also the first time that the method is used on terrain with a significant slope and using cylinders with so large diameters.

Statistical analysis of data

The data were analised using statistical tests from the R packages (R Development Core Team, 2004). Kolmogirov-Smirnov or χ^2 tests were performed to test the hypothesis of normal distribution of the data. When appropriate, i.e. independent normal distribution for residuals, along with equality in variances, Student t-tests were performed to study the degree of significance of differences in averages amongst different factors (pedology and land use classes). Otherwise, non parametrical tests (Kruskal-Wallis / Wilcoxon tests) were performed. Results are presented in terms of the critical probability p that quantifies the risk to be wrong when rejecting the null hypothesis (no effect and no difference). If $p<0.05$ (respectively <0.10), then the hypotheses of equality of mean/variance/distribution is rejected at the 5% (respectively 10%) level and the difference amongst classes can be considered as significant at this level.

Author-produced version of the article published in Hydrological Processes, vol. 24, n° 17
The original publication is available at http://www3.interscience.wiley.com doi : 10.1002/hyp.7640

The replicates were considered as independent samples in the statistical analysis. Except three points, the sampled points within the same field were distant from more than 20 m. The distance between fields was more than 50-100 m. In the recent synthesis proposed by van der Keur and Iversen (2009), soil porosity is reported to have a spatial correlation ranging from 0 to about 75 m from three different studies. Saturated hydraulic conductivity spatial correlation is reported to range between 0 and about 40 m in six studies. These figures and the fact that most of the points were collected in different fields, even at the same site, justify our independence hypothesis of the measurement points.

RESULTS

In this section, we discuss the results in terms of soil texture, soil porosity, fitting of the infiltration tests. Then, results of the single ring infiltration tests, and of mini-disk infiltration tests, are discussed. Finally, results are summarised in terms of retention and hydraulic conductivity curves. A mapping of the topsoil surface properties over the Mercier catchment is also proposed.

Soil texture

The soil particle size distribution was measured using 28 samples of the topsoil. Figure 3a presents the results for clay, fine and coarse silt, fine and coarse sand. Table II summarizes these results as well as those of the shape parameters n and η of the retention and hydraulic conductivity curves. Figure 4 presents all the sample points in the USDA textural triangle. It shows that all the topsoil A horizons belong to the sandy loam soil class except one loam, one silty clay loam and two loamy sands. However, the variability of texture within the sandy loam class is quite large. The soils have generally a coarse texture, with an average sand content of 67.5%. The coefficient of variation of the sand fractions is about 20%. The clay content is 13% on average, with a lower coefficient of variation (14%). The silt content is about 20% on average, with the largest coefficient of variation (30%). The χ^2 goodness of fit test showed that the Gaussian distribution was acceptable for all the fractions (p>0.10). The Kruskal-Wallis test showed no significant differences in distribution in terms of Soil Cartographic Unit (SCU) for all the fractions except the fine sand fraction at the 5% level (p=0.02), the coarse silt fraction (p=0.09), and the coarse sand fraction (p=0.094) at the 10% level.

The organic matter content shows a high variability with a coefficient of variation of about 50% ranging from 2 to 13%, with the highest content in forest soils and pasture. The Gaussian distribution is also acceptable for organic matter (p=0.57). The Kruskal-Wallis test showed significant differences at the 10% level in terms of land use (p=0.08) but not in terms of (SCU) (p=0.17).

Table II also provides the shape parameters of the retention and hydraulic conductivity curves n and η. The n parameter should be larger than two so that m derived from Eq.(3) is positive. The average value of n (2.17) is therefore quite low and its variability is small (CV of about 2%). The η parameter has a mean value of 15.2 and a higher coefficient of variation (20%). The Gaussian distribution was found acceptable for n at the 5% level (p=0.07), and η at the 10% level (p=0.12). The n and η parameters have small coefficient of variations and the average value can be considered as representative of the catchment. However, this hypothesis must be verified using the distributed hydrological model. These parameters control the decay of the retention and hydraulic conductivity curves when the soil dries out, through a power function. And some authors have reported a high sensitivity of water balance components to small variations of n (e.g. Braud, 1998; Boulet *et al.*, 1999).

Dry bulk density and porosity

The dry bulk density estimated using the 0-2.5 cm height and the 0-5 cm height cylinders are compared in Figure 5a. The correlation is good, R^2=0.85 ($p < 10^{-6}$, 19 samples), with values of the dry bulk density in general lower when using the smaller cylinders. This result is not surprising as the 0-2.5 cm height samples consist almost exclusively of topsoil which contains more organic matter and vegetation residues. The average dry bulk density of all the samples was 1078 kg m^{-3} (± 318). This value is quite low. Soil 704, classified as loamy sand to clayey sand presents the highest density of 1330 kg m^{-3} (± 281). In contrast soil 1031 (loamy sand from tuffs) shows the lowest average of 709 kg m^{-3} (± 135).

The statistics of the 0-5 cm height values with respect to land use classes are presented in Table III, as well as the statistics of organic matter and porosity (see also Figure 3b). As expected, the highest organic matter contents are observed in permanent pasture and forest soils whereas the lowest values are encountered in the cultivated fields. Points with the highest organic matter content are associated with the lowest dry bulk density and highest porosity. This is illustrated in Figure 5b which shows the correlation between dry bulk density and organic matter content. The correlation is significant with R^2=0.54 (p = 10^{-5}, 27 samples).

The statistics of organic matter and dry bulk density with respect to pedologic units (SCU) are not shown in Table III as the Kruskal-Wallis test indicated that differences amongst classes were not significant at the 10% level (p=0.18) when soil 1031, exhibiting the lowest values, was excluded. The differences in terms of land use were significant. The Wilcoxon rank sum test (or Mann-Witney test) was performed for all the combinations of two land use groups. It allowed the proposition of three main classes of dry bulk density by gathering the classes where the p-value was higher than 0.1. One class could be identified easily corresponding to forest soils (broad leaved and coniferous forests) with the lowest dry bulk density and highest organic matter content (class DB1). For the two other classes, it was not so easy to distinguish between land uses, especially for land use 4 (bare soil after ploughing). Based on the largest p values, we defined the two other classes as follows: permanent pasture, clearing and small woods for class DB2, with intermediate dry bulk density; and cultivated pasture, crops and orchards for class DB3 with the highest dry bulk density. The statistical properties of the variables with respect to these new classes are presented in Table IV. We verified *a posteriori* that the classification was relevant, as the *p* value amongst any pair of classes was lower than 10^{-6}. A cluster analysis of the points, described using dry bulk density and organic matter content, led to the same three main classes as the method presented above. It strengthens the conclusion that land use has a strong impact on the topsoil dry bulk density. This can be explained by agricultural practices and machines that induce a higher dry bulk density corresponding to a soil compaction.

The same classes are obtained for porosity, as the latter is a decresing function of the dry bulk density.

We mentioned before that the final water content θ_0 was assumed to be equal to the saturated water content. To assess the consistency of this hypothesis, we calculated the ratio θ_0/ε. Three points had values higher than 1 and the final water content was thus set to the porosity. The range of the values was large: [0.35-1]. Values lower than 0.4 were associated to forest or small woods soils with a high organic matter content and a high porosity. The hydrophobic effect of organic matter could also influence these results. The average of the ratio was 0.7 ± 0.18 (57 points), a value much lower than the values commonly reported in the literature 0.8-1 (Rogowski, 1971). Table IV shows the values of this ratio per dry bulk density classes (DB1, DB2 and DB3). It shows a large range of values for the three classes with a range of [0.3-1.0] in all cases. Contrary to what happens for dry bulk density and porosity, the differences amongst the three classes are not significant for this ratio with values of the Wilcoxon rank sum test *p*-values larger than 0.65.

Fitting of single ring and mini-disk infiltration tests

Due to the experimental protocol (small oscillations of the water surface just after removing the plastic sheet), there were some uncertainties on the initial level within the cylinder. Furthermore, due to the terrain slope (from zero to about 10%), the initial value was not always equal to the nominal value corresponding to the water volume divided by the cylinder surface, i.e. 95.5 mm. The initial level was thus adjusted manually to ensure data consistency. In order to assess *a posteriori* the reliability of the fitted parameters for the two methods, we calculated the gravitational time given by Eq. (9). For 76% of the SR infiltration test and 65% of the MDI tests, the total infiltration time was larger than the gravitational time. Thus the asymptotic regime could be assessed with a good accuracy for these tests and all the data were processed using both Eq. (6) and Eq. (10). On the other hand, the short time infiltration Eq. (6) could be valid for only a very few points, leading to less robust estimation of sorptivity. This is illustrated on Figure 6a where only the 6 first data points fit the short time model and the other points fit the asymptotic equation. In this case, the influence of capillary force was very short and the gravitational time was reached after about 100 s. In this case, the sorptivity was estimated with only a small number of points which can be detrimental to the robustness of the optimization, but is theoretically adequate. When the maximum infiltration time was lower than the gravitational time, the short time model of Eq. (6) was valid for the whole infiltration test duration. In this case, the estimated sorptivity was numerically robust, whereas the estimation of the asymptotic regime was less easy. This is illustrated in Figure 6b where the slope of the long time infiltration curve (Eq.(10)) is parallel to the asymptotic infiltration equation (dashed line) and the data fit the short time model up to the end. It shows that the gravitational time was not yet reached. For these infiltration tests, the effect of the terrain slope on the results was thus minimum and the estimation of sorptivity was robust (Chen and

Young, 2006). Figure 6 illustrates the SR data but the same kind of results was obtained for the mini-disk infiltration data.

For the SR infiltration tests, the average gravitational time was 6 min ± 14 min and, for the MDI infiltration tests, the average was 60 min ± 138 min. It can be compared to the infiltration test duration which was 10 min ± 19 min for SR and 33 min ± 35 min for the MDI infiltration tests. Capillary effects were thus very short for the positive head infiltration tests, whereas they lasted much longer for tension-disk infiltration. In both cases however, the use of the BEST method for optimization allowed to exploit at best the available data both before and after the gravitational time was reached.

Single ring infiltration tests

Table V shows the results of the infiltrated depth and maximum infiltration time. The values show that the infiltrated depth was close to the nominal value (volume of water / cylinder surface = 95.5 mm) with a median of 90 mm. Only four points did not work very well and had a much smaller infiltration depth. The slope of the terrain over which the cylinders were installed was responsible for this difference between the real and nominal infiltrated depths. In terms of maximum infiltration time, the range was from a few seconds (15 s) to 114 min for the longest test, with an average value of about 10 min and a median of about 3 min. Thus half of the infiltration tests took place in less than 3 min, which was very rapid and allowed to minimize the possible effect of slope on the infiltration. The high infiltration rates can also be related with preferential flow, which is not sensitive to slope effect. Only three tests had duration larger than 45 min, and two of them were located on flat areas.

As in de Condappa (2005), we introduce the ratio

$$L = I_{max}/t_{max} \quad (15)$$

where I_{max} (mm) is the maximum infiltrated depth and t_{max} (s) is the time to infiltrate this quantity. As all the infiltration tests had about the same maximum infiltrated quantity, this ratio could be used to rank the infiltration tests in terms of "infiltration capacity". The corresponding statistics are also provided in Table V. The average value is about 56 mm min^{-1} and the median 27 mm min^{-1}. These values show very high infiltration capacity for the catchment.

The statistics of estimated sorptivity and saturated hydraulic conductivity are provided in Table III categorized in terms of land use. As for dry bulk density, differences in K_s were not found significant in terms of pedology, with a value of the Kruskal-Wallis test of p=0.14. Significant differences were found in terms of land use. Three main classes could be identified (Figure 7). One class, class KS1, could be distinguished clearly. It was composed of land use 6 and 9 (broad leaved forest and small woods) with the highest saturated hydraulic conductivity and sorptivity (Table VI). The other land use classes could not be distinguished so easily and were defined based on the largest p values. Class KS2 includes land uses 2, 4, and 7 (cultivated pasture, bare soil after ploughing and clearing) with the lowest saturated hydraulic conductivity and sorptivity (Table VI). Finally class KS3 contains the other land uses (1, 3, 5, 8), namely permanent pasture, crops – wheat stubble and orchards-, and coniferous forest, with intermediate saturated hydraulic conductivity (Table VI). We verified *a posteriori* that the differences in distribution remained significant for both variables with the new classes with p-values of the Wilcoxon rank sum test lower than 0.006. Table VI also provides the statistics of the h_{VG} parameter. No significant differences amongst land use classes was found for h_{VG} with p-value of the Wilcoxon-test larger than 0.2. The value for h_{VG} is then considered as the same for all the KS and DB classes.

The classes in terms of saturated hydraulic conductivity are different from the classes identified for dry bulk density. In particular, coniferous forest and broad leaved forests were in the same group for dry bulk density. It is not the case for saturated hydraulic conductivity, which shows that organic matter content and dry bulk density are not the only factors influencing K_s.

Tension-disk infiltration tests and comparison between the two methods

At first, data analysis was conducted using traditional methods as described in Smiles and Knight (1976) or Vandervaere et al. (2000a). These methods fit only the short to medium time infiltration model of Eq. (6) and only a small amount of the data could be used. The estimation was not robust and mostly produced negative hydraulic conductivity values. This was not surprising, given the small cylinder radius and short transient stage of infiltration. Indeed, Vandervaere et al. (2000b) showed that, in these experimental conditions, their ST (single test) method was not recommended. The results are therefore not discussed below. We saw that the BEST method uses the whole infiltration test data, including the asymptotic regime. It allowed the derivation of reliable sorptivity and hydraulic conductivity estimates for 39/43 MDI infiltration tests. The rejected tests were in general conducted in forest or permanent pasture, where the impact of macropores might have been large and where the size of the apparatus (45 mm in diameter) did not allow aggregation of the soil heterogeneity. Table VI presents the statistics of the parameters derived from the mini-disk infiltrometer for the three classes identified for saturated hydraulic conditions. As expected, sorptivity and hydraulic conductivity were larger for the SR than for the MDI infiltration tests. The Wilcoxon rank sum tests showed that differences in distribution amongst KS classes was not significant for sorptivity and only significant for class KS3 for hydraulic conductivity. The impact of land use change on hydraulic properties was thus most pronounced at saturation. Table VI also provides the ratio between K_s and *K(-20 mm)*. The most striking result was the sharp increase of hydraulic conductivity from near saturation (-20 mm of water pressure) to

Author-produced version of the article published in Hydrological Processes, vol. 24, n° 17
The original publication is available at http://www3.interscience.wiley.com doi : 10.1002/hyp.7640

saturation with a ratio between the averages larger than 500, and a ratio between the median of 46.

Retention and hydraulic conductivity curves

All the results presented in the paper can be summarized by showing the retention and hydraulic conductivity curves typical for the combination of the DB and KS land use classes. They are shown in Figure 8 where average values of shape parameters from Table II, average values of saturated water content (calculated as average porosity times average θ_s/ε ratio) from Table IV and averages values of h_{VG}, K_s and *K(-20 mm)* in Table VI were used. The three retention curves differ mainly in saturated water content, as the same values of h_{VG} and n are used and each curve is associated with one of the DB classes. For the hydraulic conductivity curves, the Brooks and Corey model (Eq. (4)) was applied for water content lower than the value at h=-20 mm. Between this value and saturation a linear relationship between the natural logarithm of conductivity versus water content was assumed, as previously done to take into account the effect of macropores (Olioso *et al.*, 2002). A more comprehensive model, as the one proposed by Jarvis (2009) could be also be used to represent the sharp increase in hydraulic conductivity when moving from near-saturation to saturation.

Then one curve should be drawn for the various possible combinations of DB and KS classes. Below -20 mm for h, and the corresponding value for θ, the curves $K(\theta)$ differ only due to differences in saturated water contents – the same value is used for the parameter η and there are only small differences between *K(-20mm)* for a given DB class -. Therefore, only three curves can be distinguished, that correspond mainly to the DB classes, Between -20 mm of pressure and the saturation, the $K(\theta)$ curves differ also because of differences in the saturated hydraulic conductivity values K_s. Briefly, the water retention curve are only DB classes dependent and the hydraulic conductivity *K(θ)* are both DB and KS classes dependent.

The differences in saturated hydraulic conductivities identified amongst land use are only influential on a small part of the curves, i.e very close to saturation. The accurate determination of saturated water content (and therefore of dry bulk density) is shown to be the most important point to get accurate description of soil hydraulic properties over the whole range of water content. As we have shown that dry bulk density is highly related to organic matter content, these differences can be assessed quite easily in the field.

Mapping of topsoil hydraulic properties

From the results presented previously, a preliminary mapping of topsoil hydraulic properties over the Mercier catchment can be proposed.

In our case study, we have shown that the soil texture is quite homogeneous and that the variability of the shape parameters of the retention and hydraulic conductivity curves, n and η, is low. As a first approximation, these parameters are assumed constant over the whole catchment. A more refined map could be obtained by mapping first the clay, sand, and silt contents, using for instance the kriging technique. The shape parameters n and η could then be derived from the soil texture, as done in this paper (see also Lassabatère *et al.,* 2006).

The major outcome of our study is to show that soil porosity, saturated water content and saturated hydraulic conductivity, are mostly determined by land use. A land use map can therefore be used for the mapping of those parameters. In our study catchment, the land use field survey has shown that the accuracy of the Corine land cover map was too low to properly distinguish between the relevant land uses, especially crops. A more detailed land use map is therefore required. It can be derived from high resolution aerial photographs or satellite imagery. Such mapping is in progress on the Yzeron catchment (Béal *et al*., 2009) but was not available at the time of the field survey. For the Mercier catchment, a detailed map was digitalized from aerial photographs (IGN BD ORTHO 2003, updated using the IGN BD ORTHO 2008) and corrected using the cadastre for urbanised areas. This map was reclassified for the representation of topsoil hydraulic properties. This classification combines the DB classes of Table IV and the KS classes of Table VI. The correspondence between the original land use map and the reclassified one is given in Table VII. The resulting map is shown in Figure 9 where non sampled areas appear in white colour. For each DB-KS class, one value of porosity, saturated water content and hydraulic conductivity can be affected using for instance the average of the DB classes and the media of the KS classes (Table VII).

DISCUSSION

Sampling strategy

The sampling strategy is very important for an efficient mapping of the hydraulic parameters. It has been pointed out as a key question by Park and van de Giesen (2004). The question of sampling is especially relevant when dealing with a large catchment such as the Mercier catchment (7 km^2) (published studies are often related to catchments of less than 1 km^2). In previous works performed using the *Beerkan* method, on much larger catchments, a regular grid sampling was used. Such a strategy was used during the EFEDA project on a 10x10 km^2 area in Central Spain (Braud *et al.*, 2003). A regular grid (3.5 km resolution) complemented by a transect with a 20 m spacing, was also used during a field campaign conducted in the Donga catchment (580 km^2) in Benin (Varado *et al.*, 2006). Analysis of the Benin data showed a spatial correlation of about 50 to 100 m for the saturated hydraulic conductivity and no correlation on the 3.5 km grid. On the other hand, it was shown that average values were significantly different when the data were classified according to pedological units. A regular grid sampling does not allow the valorization of existing information such as pedology and land use. The sampling strategy adopted in this stydy was focused on the future hydrological modeling, where the hydrological units, coined as hydro-landscapes by Dehotin and Braud (2008), are chosen to be as homogeneous as possible with respect to soil, land use and other factors such as slope or the Beven topographic index. The pre-selection of sites based on the combination of pedology and land use information, as well as accessibility, was found efficient in terms of duration of the field campaign and use of human resources. It allowed the sampling of pedology/land use combinations representing a significant fraction of the catchment area. As shown in Figure 9, the characterization of artificialized areas is missing, but lots of practical problems (mainly difficult access to private properties) prevent an efficient sampling of these areas. As much as possible, the literature should be used instead.

Results of the infiltration tests

In this study two types of infiltration test were used to assess the hydraulic properties of the Mercier catchment topsoil A horizon. For a given location, the results of the three SR infiltration tests replications were in general very consistent whereas the variability was larger for the MDI infiltration tests. The difference in sampling surface between both devices may be the explanation. Indeed, the large cylinder diameter of the SR tests averaged most of the soil heterogeneity and removed much of the spatial variability due to inadequate sampling of macropore effect. The large diameter of the cylinder also filtered out the effects of terrain slope and vegetation. It reduces the effect of the heterogeneity of soil structure and texture and the parameters estimated from the infiltration tests are associated with this weighing of surface heterogeneities. The obtained values can therefore be considered representative of the field. On the other hand, the sampling surface of the MDI infiltrometer was very small and therefore these were much more sensitive to soil variability and heterogeneity of the topsoil A horizon. However, given the slope and the surface heterogeneity, it would have been difficult to use a large diameter for the mini-disk: this apparatus requires a flat surface to ensure stability and a good contact with the membrane. This would have required digging through the slope, that would have disturbed the soil surface and would not have been representative of the topsoil anymore. Finally, the two types of infiltration tests were complementary and well adapted to the field conditions on this highly structured soil.

In addition, the positive head infiltration test allowed a characterization of saturated conditions, whereas the tension-disk data provided information on near-saturated hydraulic conductivity (-20 mm of water pressure), and illustrated the sharp increase in conductivity when moving from near-saturated to saturated conditions. This difference can be explained by the activation, at saturation, of a macropore network related to the high organic content, and a higher root system density and soil fauna activity in natural vegetations (broad leaved forest, permanent pasture). A review of the effect of macropores on water flow has been proposed by Beven and Germann (1982). They reports an increase of the infiltration capacity of soils with macropores. In the paper by Zhou *et al.* (2008, Table 5, Fig. 1), a ratio of about 10 between hydraulic conductivity at -30 mm of pressure and saturation is reported for woodland, cropland, pasture and urban land uses. In the paper by Schwartz *et al.* (2003, Fig. 3) the ratio between hydraulic conductivity at -20 mm of pressure and saturation is of about 2. In these two papers saturated hydraulic conductivity was obtained using tension-disk infiltrometers with a pressure of 0 m, which are shown by Reynolds *et al.* (2000) to provide lower estimates of saturated hydraulic conductivity than pressure infiltrometers Our values are therefore consistent with the literature, although the values of the ratio is around 50 in our study.

The BEST method used in data interpretation was found robust and allowed us to obtain results even in adverse conditions (gentle slope, very rapid infiltration, and dense vegetation detritus cover in some cases). The strength of the method is its ability to exploit both the short

Author-produced version of the article published in Hydrological Processes, vol. 24, n° 17
The original publication is available at http://www3.interscience.wiley.com doi : 10.1002/hyp.7640

and long term ranges of the infiltration tests in order to describe at best the data. It also provided physical results when traditional methods, based only on the short time infiltration regime, failed. The method is applicable for both positive head and tension-disk infiltration data, provided the contact layer has no significant influence on the early stages of infiltration. When positive head is applied, the method provides an estimate of the normalization parameter for the pressure and thus a complete description of both the retention and hydraulic conductivity curves, which is not the case of traditional analysis methods. However, several limitations of the methods have been identified. Xu et al. (2009) underline that the BEST method is not effective when the initial water content is not sufficiently different from the final water content. However, this restriction apply to all the methods of analysis because the difference in water content appears in the denominator of Eq. (6). Another limitation is related to the use of two different equations during the analysis which requires the determination of the number of points where the small time infiltration equation is valid, through a specific BEST routine (Eq. (7)). This choice influences the final sorptivity value and is therefore important. The approximation provided by Eq.(6) was shown to be adequate for modeling *Beerkan* infiltration experiments, provided its use is restricted to valid intervals (Lassabatere *et al.*, 2009). Improvement of the BEST method were recently proposed for specific soils (Yilmaz et al., 2010) but were not used here. Based on the validation of the full integration equation (Lassabatere *et al.*, 2009), work is in progress in order to directly solve the full infiltration equation proposed by Haverkamp *et al.* (1994). The results presented in the paper were partly verified using this new solution, which strengthens the confidence in the conclusions. More theoretical and numerical studies should be conducted to better assess the impact of slope on the final results.

Impact of land use on topsoil hydraulic properties

Our study also highlighted the impact of land use on soil structural parameters, whereas the impact of pedology was not found so significant in our case study. Three land use classes were identified, leading to significant differences in dry bulk density and porosity. These classes were highly related to the organic matter content and therefore to the land use insofar as organic matter content is lower in cultivated lands than in natural areas (forests, permanent pastures). Lal (1996) reported an increase in dry bulk density when forest was replaced by cultivated lands, which is consistent with our findings.

In our study, three further land use classes were identified with significant differences in saturated hydraulic conductivity and sorptivity. However, these classes were not significantly different in terms of near-saturated hydraulic conductivity, showing that the classes were probably related to macropores. Once again, the appearance of a dense macropore network is favoured by fauna activity and the dense root network in natural vegetations. Several authors have reported results showing the impact of land use on soil hydraulic properties. For instance, Marshall *et al.* (2009) report higher saturated hydraulic conductivity of soil beneath tree hedges than in agricultural fields, with a ratio of the both of about 3. Reynolds *et al.* (2000, Table 4) report values of saturated hydraulic conductivity measured using pressure infiltrometers. The geometric mean values on natural woodlot are 2 to 10 times larger than those under conventional and no-tillage practices. More stable soil structure and increased biological activity might explain the larger hydraulic conductivity in forest, permanent pasture or minimum tillage systems (Bodhinayake and Si, 2004). Stolte *et al.* (2003) report that the permanent land use (forest, orchard, wasteland, shrub) showed a greater heterogeneity of saturated hydraulic conductivity than the arable areas and the values were significantly higher in permanent land use than in cultivated areas, as in our study. This was probably due to more macropores, associated with the activity of fauna and roots in the permanent system than in arable land. Such changes in topsoil hydraulic properties are very important for hydrological processes such as surface runoff but also groundwater, and water quality. They modify the hydrological response in terms of water balance components and their annual temporal variability (e.g., Fohrer *et al.*, 2005; Bormann *et al.*, 2007). Hibbert (1967) and Bosch and Hewllet (1982) concluded that a reduction of the forest cover increases water runoff.

Our data were collected in autumn, but especially for agricultural fields, our results should be complemented by a monitoring of the time evolution of soil hydraulic properties, as suggested by several studies. This fact is especially relevant for agricultural fields where soil properties are modified regularly by agricultural practices such as ploughing, sowing, etc…(Zhou *et al.*, 2008; Bormann and Klassen, 2008; Le Bissonais *et al.*, 2005; Schwarts *et al.*, 2003; Mubarak *et al.*, 2009).

CONCLUSIONS

The results presented in this paper show that using an adequate spatial sampling taking into account pedology, and especially land use, it was possible to document the spatial variability of soil hydraulic properties of a small catchment of 7 km^2. The use of two types of infiltration tests, namely positive head and tension disk infiltration tests, combined with particle size data analysis and porosity measurements, allowed the derivation of estimates of the retention and hydraulic conductivity curves. Positive head and tension-disk data provided complementary information about saturated and near-saturated hydraulic conductivity of the topsoil A horizon. They highlighted a sharp increase of hydraulic conductivity when moving from near-saturated (-20 mm of water pressure) to saturated conditions. This fact could be related to the existence of macroporosity, mainly related to land use management. Therefore, the monitoring of both saturated and near-saturated hydraulic conductivity can provide information on the long term impact of land use on soil hydraulic properties.

In addition, the study revealed a significant impact of land use on dry bulk density and porosity, as well as on saturated hydraulic conductivity. This result opens perspectives for the spatialization of soil hydraulic conductivity. Traditionally, in distributed hydrological models, soil hydraulic properties are specified using pedo-transfer functions that rely mainly on soil texture and sometimes on porosity (or dry bulk density). These functions are generally fitted on a limited data set, often obtained in the laboratory, and might not be adapted to *in situ* soil conditions. Our study highlights the impact of land use on soil hydraulic properties and confirms the results of other authors such as those mentioned in the *Discussion* section. This should also be taken into account in the mapping of soil hydraulic properties for hydrological modelling. We have shown that a high resolution land use map is very valuable and can be used for this purpose.

ACKNOWLEDGEMENTS

The soil data base was provided by SOL INFO RHONE-ALPES, sira@rhone-alpes.chambagri.fr, http://www.rhone-alpes.chambagri.fr/sira/. The study was funded by the by the French Agence Nationale de la Recherche (ANR) under contract n° ANR-07-VULN-01. The stay of the first author at Cemagref was funded by Queretaro University, Mexico and Cemagref. Jean-Pierre Vandervaere provided useful comments on the interpretation of tension disk infiltration tests. We also thank two anonymous reviewers for their suggestions which help improve the quality of the paper.

REFERENCES

Béal D, Gagnage M, Jacqueminet C, Kermadi S, Michel C, Jankowfsky S, Branger F, Braud I. 2009. Cartographie de l'occupation du sol pour la modélisation hydrologique spatialisée du cycle de l'eau en zone péri-urbaine, Proceedings 2ème atelier SIDE2009 Systèmes d'Informations et de Décision pour l'Environnement, Biramonte S, Miralles A, Pinet F (eds), Toulouse, France, May 26 2009, 10 pp. Available at http://eric.univ-lyon2.fr/~sbimonte/side2009.html, consulted on 2010/01/15.

Beven K, Germann P. 1982. Macropores and water flow in soils. *Water Resources Research*, **18(5)**: 1311-1325.

Bodhinayake W, Si BC. 2004. Near-Saturated surface soil hydraulic properties under different land use in the St Denis National Wildlife Area, Saskathchewan, Canada. *Hydrological Processes* **18**: 2835-2850.

Booth DB, Hartley D, Jackson R. 2002. Forest cover, impervious-surface area, and the mitigation of stormwater impacts. *Journal of the American Water Resources Association*, **38(3)**: 8356-845.

Bormann H, Breuer L, Gräff T, Huisman JA. 2007. Analysing the effects of soil properties changes associated with land use changes on the simulated water balance: A comparison of three hydrological catchment models for scenario analysis. *Ecological Modelling*, **209(1)**: 29-40.

Bormann H, Klassen K. 2008. Seasonal and land use dependent variability of soil hydraulic and soil hydrological properties of two Nothern German soils. *Geoderma* **145**: 295-302.

Bosch JM, Hewllet PM. 1982. A review of catchment experiments to determine the effect of vegetation changes on water yield and evapotranspiration. *Journal of Hydrology* **55**:3-23.

Boulet G, Kalma JD, Braud I, Vauclin M. 1999. An assessment of effective parameterization of soil physical and land surface properties in regional-scale water balance studies. *Journal of Hydrology* **217**: 225-238.

Bras RL, Perkins FE. 1975. Effects of urbanization on catchment response. *J. of Hydraulics Division* **101** HY3: 451-466.

Braud I. 1998. Spatial variability of surface properties and estimation of surface fluxes of a savannah. *Agricultural and Forest Meteorology* **89(1)**: 15-44.

Braud I, de Condappa D, Soria J, Haverkamp R, Angulo-Jaramillo R, Galle S, Vauclin M. 2005. Use of scaled forms of the infiltration equation for the estimation of unsaturated soil hydraulic properties (Beerkan method). *European Journal of Soil Science* **56**: 361-374. DOI: 10.1111/j.1365_2389.2004.00660.x.

Braud I, Haverkamp R, Arrué JL, Lopez MV. 2003. Spatial variability of soil surface properties and consequences on the annual and monthly water balance of a semi-arid environment (EFEDA experiment). *Journal of Hydrometeorology* **4(1)**: 121-137.

Brooks RH, Corey CT. 1964. Hydraulic properties of porous media. *Hydrological Paper* **3**. Colorado State University, Fort Collins, CO.

Burdine NT. 1953. Relative permeability calculations from pore size distribution data. *Transactions of the American Institute of Mining, Metallurgical, and Petroleum Engineers* **198**: 71-77.

Chen L, Young MH. 2006. Green-Ampt infiltration model for sloping surfaces. *Water Resources Research* **42**: W07420, doi:10.1029/2005WR004468

Childs EC, Collis-George C. 1950. The permeability of porous media. *Proceedings of the Royal Society London Series A* **201:** 393-405.

Chocat B, Krebs P, Marsalek J, Rauch W, Schilling W. 2001. Urban drainage redefined: from stormwater removal to integrated management. *Water and Science Technology* **43**:61-68.

Clapp RB, Hornberger GM. 1978. Empirical equations for some soil hydraulic properties. *Water Resources Research* **14(4)**: 601-604.

Cosby BJ, Hornberger, GM, Clapp RB, Ginn TR. 1984. A statistical exploration of the relationships of soil moisture characteristics to the physical properties of soils. *Water Resources Research* **20(6)**: 682-690.

de Condappa D. 2005. Etude de l'écoulement d'eau à travers la zone non-saturée des aquifères de socle à l'échelle spatiale du bassin versant. Application à l'évaluation de la recharge au sein du bassin versant de Maheshwaram, Andhra Pradesh, Inde, Université Joseph Fourier, Grenoble, France, 22 Avril 2005, 355 pp.

de Souza ES, Antonino ACD, Angulo-Jaramillo RA, Netto AM, Montenegro SMGL, da Silva EB. 2008. Spatial variability of hydrodynamic parameters in two agricultural plots in Paraiba state – Brazil, *Reivista, Brasileira de ciencia do solo* **32(5)**: 1795-1804.

Dehotin J, Braud I. 2008. Which spatial discretization for distributed hydrological models? Proposition of a methodology and illustration for medium to large scale catchments. *Hydrology and Earth System Sciences* **12**: 769-796.

Desbordes M. 1989. Principales causes d'aggravation des dommages dus aux inondation par ruissellement superficiel en milieu urbanisé. *Bulletin hydrologie urbaine*- SHF, Paris, **4** : 2-10.

Fohrer N, Haverkhamp S, Frede H. 2005. Assessment of the effects of land use patterns on hydrological landscape functions: development of sustainable land use for low mountain range areas. *Hydrological Processes* **19** : 659-672.

Gnouma R. 2006. Aide à la calibration d'une modèle hydrologique distribué au moyene d'une analyse des processus hydrologiques: application au basin versant de l'Yzeron. Thèse Doctoral. Institut National des Sciences Appliquées de Lyon. France, 412 pp.

Gutmann ED, Small EE. 2005. The effect of soil hydraulic properties versus soil texture in land surface models. *Geophysical Research Letters* **32**: L02402, doi: 10.1029/2004GL021843.

Haverkamp R, Bouraoui F, Angulo-Jaramillo R, Zammit C, Delleur JW. 1998. Soil properties and moisture movement in the unsaturated zone. In: *CRC Groundwater Engineering Handbook*, Delleur JW (ed), CRC Press, Boca Raton, Florida: 5.1-5.50,.

Haverkamp R, Leij FJ, Fuentes C, Sciortino A, Ross PJ. 2005. Soil water retention: I. Introduction of a shape index. *Soil Science Society of America Journal* **69**: 1881-1890, doi: 10.2136/sssaj2004.0225.

Haverkamp R, Ross PJ, Smettem KRJ, Parlange JY. 1994. Three-dimensional analysis of infiltration from the disk infiltrometer 2. Physically based infiltration equation. *Water Resources Research* **30(11)**: 2931-2935.

Herman S, Mertens J, Timmerman A, Feyen J. 2003. Comparison of tension infiltrometer, single-ring pressure infiltrometer and soil core Ksat estimates on a sandy loam hillslope. EGS - AGU - EUG Joint Assembly, Abstracts from the meeting held in Nice, France, 6 - 11 April

Hibbert AR. 1967. Forest treatment effects on water yield. In the International Symposium on Forest Hydrology, Pensylvania , September 1965, Sopper WE, Lull HW (eds.) Pergamon; Oxford.

Islam N, Wallender WW, Mitchell JP, Wicks S, Howitt RE. 2006. Performance evaluation of methods for the estimation of soil hydraulic parameters and their suitability in a hydrologic model. *Geoderma* **134(1-2)**: 135-151.

Jarvis N. 2009. Near-saturated hydraulic properties of macroporous soils. *Vadose Zone Journal* **7**: 1302-1310.

Lafont M, Vivier A, Nogueira S, Namour P, Breil P. 2006. Surface and hyporheic oligochaete assemblages in a French suburban stream. *Hydrobiologia* **564(1)**: 183-193.

Lal R. 1996. Deforestation and land-use effects on soil degradation and rehabilitation in western Nigeria. I. Soil physical and hydrological properties. *Land degradation and development* **7**: 19-45.

Lassabatère L, Angulo-Jaramillo R, Soria Ugalde JM, Cuenca R, Braud I, Haverkamp R. 2006. *Beerkan* estimation of soil transfer parameters through infiltration experiments. *Soil Science Society of America Journal* **70**: 521-532.

Lassabatère L, Angulo-Jaramillo R, Soria Ugalde JM, Simunek J, Haverkamp R. 2009. Analytical and numerical modeling of water infiltration experiments. *Water Resources Research* **45**: W12415.

Le Bissonnais Y, Cerdan O, Lecomte V, Benkhadra H, Souchere V, Martin P. 2005. Variability of soil surface characteristics influencing runoff and interrill erosion. *Catena* **62**: 111-124.

Marsalek J, Jiménez-Cisneros BE, Karamouz M, Malmquist PA, Gldenfum J, Chocat B. 2007. Urban water processes and interactions. UNESCO IHP-VI program, UNESCO, Paris, 239 pp.

Marshall MR, Francis OJ, Frobrook ZL, Jackson BM, McIntyre N, Reynolds B, Solloway I, Weather HS, Chell J. 2009. The impact of upland land management on flooding: results from an improved pasture hillslope. *Hydrological Processes* **23**: 464-474.

Matteo M, Randhir T, Bloniarz D. 2006. Watershed-scale impacts of forest buffers on water quality and runoff in urbanizing environment. *Journal of the American Water Resources Association* **132**:144-152.

Mualem Y. 1976. A new model for predicting the hydraulic conductivity of unsaturated porous media. *Water Resources Research* **12,** 513-522.

Mubarak I, Mailhol JC, Angulo-Jaramillo R, Ruelle P, Khaledian M. 2009. Temporal variability in soil hydraulic properties under drip irrigation. *Geoderma* **150(1-2)**: 158-165 doi:10.1016/j.geoderma.2009.01.022.

Olioso A, Braud I, Chanzy A, Courault D, Demarty J, Kergoat L, Lewan E, Ottlé C, Prévot L, Zhao W, Calvet JC, Cayrol P, Jongschaap R, Moulin S, Noilhan J, Wigneron JP. 2002. SVAT modelling over the Alpilles-ReseDA experiment: comparing SVAT models over wheat fields. *Agronomie* **22**: 651-668.

OTHU, 2010. http://www.graie.org/othu/. Consulted on 2010/01/06.

Author-produced version of the article published in Hydrological Processes, vol. 24, n° 17
The original publication is available at http://www3.interscience.wiley.com doi : 10.1002/hyp.7640

Park SJ, van de Giesen N. 2004. Soil-landscape delineation to define spatial sampling domains for hillslope hydrology. *Journal of Hydrology* **295(1-4)**: 28-46.

Philip JR. 1969. Theory of infiltration. *Advances in Hydroscience* **5**: 215-296.

R Development Core Team, 2004.R: a language and environment for statistical computing. R foundation for statistical computing. Vienna, Austria. http://www.r-project.org/. Consulted on 2010/01/06.

Radojevic B. 2002. Méthode d'évaluation de l'influence urbaine sur le régime des crues d'un bassin versant de 130 km2. Institut National des Sciences Appliquées de Lyon, Lyon.

Randhir T. 2003. Watershed-scale effects of urbanization on sediment export: assessement and policy, *Water Resources Research* **39(6)**, 1-13.

Rawls WJ, Brakensiek DL. 1985. Prediction of soil water properties for hydrologic modelling. In: *E.B.a.W*. Jones TJ (eds), Watershed Management in the eighties. ASCE, Denver, April 30-May 1: 293-299.

Reynolds WD, Bowman BT, Brunke RR, Drury CF, Tan CS. 2000. Comparison of tension infiltrometer, and soil core estimates of saturated hydraulic conductivity. *Soil Science Society of America Journal* **64**:478-484.

Rogowski AS. 1971. Watershed physics: model of soil moisture characteristic, *Water Resources Research* **12**: 513-522.

Scalenghe R, Ferraris S. 2009. The First Forty Years of a Technosol. *Pedosphere* **19(1)**: 40-52.

Schmitt L, Grosprêtre L, Breil P, Lafont M, Vivier A, Perrin JF, Namour P, Jezequel C, Valette L, Valin K, Cordier R, Cottet M. 2008. Préconisations de gestion physique de petits hydrosystèmes périurbains : l'exemple du bassin de l'Yzeron (France). In. Actes du Colloque « La gestion physique des cours d'eau : bilan d'une décennie d'ingénierie écologique »,

Author-produced version of the article published in Hydrological Processes, vol. 24, n° 17
The original publication is available at http://www3.interscience.wiley.com doi : 10.1002/hyp.7640

Verniers G, Petit F (eds), Namur, 10-12 oct. 2007, Groupe Interuniversitaire de Recherches en Ecologie Appliquée, Laboratoire d'Hydrographie et de Géomorphologie Fluviatile, Direction des Cours d'Eau Non Navigables, Direction Générale des Ressources Naturelles et de l'Environnement - Ministère de Région wallonne : 177-186.

Schwarts R, Evett SR, Paul UW. 2003. Soil hydraulic properties of cropland compared with reestablished and native grassland. *Geoderma* **116**: 47-60.

SIRA, 2010. Sol Info Rhône-Alpes, sira@rhone-alpes.chambagri.fr - http://www.rhone-alpes.chambagri.fr/sira/. Consulted on 2010/01/06.

Smettem KRJ, Parlange JY, Ross PJ, Haverkamp R. 1994. Three-dimensional analysis of infiltration from the disk infiltrometer. 1. A capillary-base theory, *Water Resources Research* **30**, 2925-2929.

Smiles DE, Knight JH. 1976. A note on the use of the Philip infiltration equation, *Australian Journal of Soil Science* **10**: 143-150.

Sobieraj JA, Elsenbeer H, Vertessy RA. 2001. Pedotransfer functions for estimating saturated hydraulic conductivity: implications for modelling strom flow generation. *Journal of Hydrology* **251**: 202-220.

SOeS, 2010. Service de l'Observation et des Statistiques, Occupation des Sols, Corine Land Cover, http://www.ifen.fr/bases-de-donnees/occupation-des-sols-corine-land-cover.html?taille=. Consulted on 2010/01/06.

Stolte J, van Venrooij B, Zhang G, Trouwborst KO, Liu G, Ritsema CJ, Hessel R. 2003. Land-use induced spatial heterogeneity of soil hydraulic properties on the Loess Plateau in China. *Catena* **54**: 59-75.

van der Keur P, Iversen BV. 2006. Uncertainty in soil physical data at the basin scale - a review. *Hydrology and Earth System Sciences* **18**: 889-902 van Genuchten MT. 1980. A closed-form equation for predicting the hydraulic conductivity of unsaturated soils. *Soil Science Society of America Journal* **44 :** 892-898.

Vandervaere JP, Vauclin M, Elrick DE. 2000a. Transient flow from tension infiltrometers: I. The two-parameter equation. *Soil Science Society of America Journal* **64**: 1263-1272.

Vandervaere JP, Vauclin M, Elrick DE. 2000b. Transient flow from tension infiltrometers: II. Four methods to determine sorptivity and conductivity. *Soil Science Society of America Journal*, **64**: 1271-1284.

Varado N, Braud I, Galle S, Le Lay M, Séguis L, Kamagate B, Depraetere C. 2006. Multi-criteria assessment of the Representative Elementary Watershed approach on the Donga catchment (Benin) usin a downward approach of model complexity. *Hydrology and Earth System Sciences* **10**: 427-442.

Verecken H, Maes J, Darius P, Feyen J. 1989. Estimating the soil moisture retention characteristics from texture, bulk density and carbon content. *Soil Science* **148**: 389-404.

Wösten JHM. 1997. Pedotransfer functions to evaluate soil quality; In *Development in soils sciences*, Gregorich E, Carter MR (eds)., Elsevier: Amsterdam; 221-245.

Wösten JHM, Lilly A, Nemes A, Le Bas C. 1999. Development and use of a database of hydraulic properties of European soils. *Geoderma* **90**: 169-185.

Wösten JHM, Pachepsky YA, Rawls WJ. 2001. Pedotransfer functions: bridging the gap between available basic soil data and missing soil hydraulic characteristics. *Journal of Hydrolog*y **251**: 123-150.

Xu X, Kiely G, Lewis C. 2009. Estimation and analysis of soil hydraulic properties through infiltration experiments: comparison of BEST and DL fitting methods. *Soil Use and Management* **25**: 354-361.

Yilmaz D, Lassabatère L, Angulo Jaramillo R, Legret M. 2010. Hydrodynamic characterization of BOF slags through adapted BEST method. *Vadoze Zone Journal* **9**: 1-10.

Zhou X, Lin HS, White HS. 2008. Surface soil hydraulic properties in four soil series un different land uses and their temporal changes. *Catena* **73**: 180-188.

Author-produced version of the article published in Hydrological Processes, vol. 24, n° 17
The original publication is available at http://www3.interscience.wiley.com doi : 10.1002/hyp.7640

List of Figures

Figure 1: Location of the Yzeron catchment and of the two experimental sub-catchments (Mercier and Chaudanne). The grey scale shows the catchment slope with the highest values in dark and the lowest values in white. The symbols indicate the location of rainfall (points) and streamflow gauges (triangles).

Figure 2: Pedology map of the Mercier catchment (from Sol Info Rhône Alpes, SIRA, 2010). The various colors correspond to the various Soil Cartographic Units defined in Table I. The symbols show the location of the infiltration test sites, with the various symbols corresponding to the various land use defined in Table I.

Figure 3: (a) Box plot of the fine particle size fractions and organic matter content (b) Box plot of the dry bulk density and porosity of the topsoil. On the box plots, boundaries indicates median, 25^{th} and 75^{th} quantiles, the top and bottom whiskers indicate the 10^{th} and 90^{th} percentiles and the points the minimum and maximum values.

Figure 4: Presentation of the sampled points in the USDA textural triangle. The various symbols correspond to the different soil pedological units as defined in Table I.

Figure 5: (a) Comparison of dry bulk density as measured using a 0-2.5 cm and 0-5 cm height cylinder. (b) Relationship between dry bulk density and organic matter content.

Figure 6. Observed (points) and fitted cumulative infiltration data for sites 41.1 (clearing) and 31-3 (orchards). The full line is the fit of Eq. (6) for short time steps and the dashed line is the fit of Eq. (10) for large time steps. Eq. (6) was fitted to the points plotted with squares.

Figure 7. Box plots of saturated hydraulic conductivity (single ring) and hydraulic conductivity at -20 mm (mini-disk) for all the samples and the three identified classes KS1, KS2 and KS3.

Author-produced version of the article published in Hydrological Processes, vol. 24, n° 17
The original publication is available at http://www3.interscience.wiley.com doi : 10.1002/hyp.7640

Figure 8. Estimated retention curves and hydraulic conductivity curves for the combination of classes DB1, DB2, DB3. Between near-saturated and saturated hydraulic conductivity, a linear relationship on the natural logarithm of hydraulic conductivity versus soil water content was assumed. The symbols are the saturated hydraulic conductivities for the various combinations of DB and KS classes: broad leaved forest (DB1-KS1); coniferous forest (DB1-KS3); permanent pasture (DB2-KS3); clearing (DB2-KS2); small woods (DB2-KS1); cultivated pasture (DB3-KS2); crops (DB3-KS3)..

Figure 9. Mapping of soil hydraulic properties. The classes numbering is provided in Table VII. White surfaces correspond to the non sampled areas defined in Table VII.

Author-produced version of the article published in Hydrological Processes, vol. 24, n° 17
The original publication is available at http://www3.interscience.wiley.com doi : 10.1002/hyp.7640

Table I. Number of sampled points for Single Ring (SR) and Mini-Disk (MDI) infiltration tests per Soil Cartographic Unit (SCU) and land use (figures in parentheses are the percentage of the total number of points). In the land use classes, we distinguish between “permanent pasture” (in place for more than 5 years) and “cultivated pasture” (in place for only one or a few years).

SCU number or land use	Number of SR tests	Number of MDI
102 Loamy sand and clayey sand from gneiss and micaschist	15 (26%)	10 (23%)
1031 Loamy sands from tuf within a forest dominated by coniferous	6 (10%)	7 (16%)
7021 Loamy sands and clayey sands from colluvionated gneiss	15 (26%)	11 (25%)
704 Colluvions loamy sand to clayey sand with slope	6 (10%)	4 (9%)
7041 Colluvions loamy sand to clayey sand within talwegs	9 (16%)	5 (12%)
7042 Alluvions clayey-sands to sandy clays within talwegs and narrow valleys	7 (12%)	6 (14%)
Total	**58**	**43**
1 Permanent pasture	21 (36%)	14 (32%)
2 Cultivated pasture	9 (15%)	7 (16%)
3 Crop (wheat stubble)	3 (5%)	2 (5%)
4 Crop (bare soil after ploughing)	4 (7%)	3 (7%)
5 Orchards (peach, apples)	3 (5%)	2 (5%)
6 Broad-leaved forest (oaks, chestnuts)	6 (10%)	6 (14%)
7 Clearing	4 (7%)	2 (5%)
8 Coniferous forest	4 (7%)	4 (9%)
9 Small wood sometimes with ivy	4 (7%)	3 (7%)
Total	**58**	**43**

Table II. Statistics of particle size data analysis, organic matter and shape parameters of the retention and hydraulic conductivity curves, *n* and *η*. CV is the coefficient of variation. The sample size is 28. Std stands for standard deviation

	Clay content	Fine silt content	Coarse silt content	Fine sand content	Coarse sand content	Organic matter content	n	η
Unit	%	%	%	%	%	g kg^{-1}	-	-
Average	12.9	11.7	8.2	17.9	49.6	56.5	2.17	15.2
Std	4.0	3.5	2.5	3.6	10.4	26.9	0.045	3.2
Minimum	5.6	4.8	3.7	10.6	30.2	18.2	2.10	10.7
Maximum	22.7	20.1	13.7	23.8	73.4	133.0	2.26	22.8
CV (%)	13.8	29.9	30.5	20.1	21.0	47.6	2.1	21.0

Table III. Average and standard deviation (std in parentheses) organic matter content, dry bulk density, porosity, sorptivity and hydraulic conductivity derived from the single ring (SR) infiltration tests in terms of land use class.

Land use	Sample size OM	Organic matter content	Sample size dry bulk density and SR	Dry bulk density	Porosity	Sorptivity SR	Saturated hydraulic conductivity SR
Units	-	g kg^{-1}	-	kg m^{-3}	-	mm $s^{-1/2}$	mm s^{-1}
Permanent pasture	11	61.3 (10.9)	21	969 (122)	0.63 (0.05)	3.15 (2.45)	0.51 (0.75)
Cultivated pasture	4	35.6 (12.9)	9	1269 (305)	0.52 (0.11)	1.64 (0.58)	0.11 (0.08)
Crops (wheat stubble)	1	19.5 (NA)	3	1411 (24)	0.47 (0.01)	2.8 (0.76)	0.28 (0.10)
Crops (bare soil after ploughing)	1	18.2 (NA)	4	1549 (265)	0.41 (0.10)	0.84 (0.83)	0.13 (0.21)
Orchards (peach, apple)	1	28.3 (NA)	3	1472 (225)	0.44 (0.08)	3.62 (2.10)	0.40 (0.27)
Broad-leaved forest	3	88.8 (54.1)	6	676 (146)	0.74 (0.05)	4.86 (1.45)	1.32 (0.57)
Clearing	3	51 (21.2)	4	1180 (283)	0.55 (0.11)	1.16 (0.40)	0.05 (0.02)
Coniferous forest	1	84.5 (NA)	4	725 (130)	0.73 (0.05)	1.50 (0.91)	0.23 (0.15)
Small wood sometimes with ivy	3	65 (19.3)	4	1058 (292)	0.60 (0.11)	5.77 (2.12)	1.50 (0.62)
All	28	56.5 (26.6)	58	1078 (318)	0.59 (0.12)	2.87 (2.18)	0.50 (0.67)

Author-produced version of the article published in Hydrological Processes, vol. 24, n° 17
The original publication is available at http://www3.interscience.wiley.com doi : 10.1002/hyp.7640

Table IV. Statistics of organic matter content, dry bulk density, porosity and ratio (final water content/porosity) for the three main land use classes where significant differences were identified: class DB1: broad leaved forest + coniferous forest, class DB2: permanent pasture + clearing + small woods, class DB3: cultivated pasture + crop (wheat stubble) + crop (bare soil after ploughing) + orchards. Std stands for standard deviation

		Number of samples	Organic matter	Dry bulk density	Porosity	Ratio final water content / porosity
	Units	(-)	(g kg^{-1})	(kg m^{-3})	(-)	(-)
Class DB1	Average	10	103.0	695	0.74	0.66
	(Std)		(24.4)	(135)	(0.05)	(0.16)
	[Min-Max]	-	[62.6-133]	[472-817]	[0.69-0.82]	[0.32-0.81]
Class DB2	Average	29	60.5	1010	0.62	0.69
	(Std)		(13.6)	(185)	(0.07)	(0.17)
	[Min-Max]	-	[26.5-86.3]	[685-1424]	[0.46-0.74]	[0.30-1.0]
Class DB3	Average	19	30.7	1382	0.48	0.70
	(Std)		(12.3)	(270)	(0.10)	(0.18)
	[Min-Max]	-	[18.2-53.3]	[846-1852]	[0.30-0.68]	[0.35-1.0]

Author-produced version of the article published in Hydrological Processes, vol. 24, n° 17
The original publication is available at http://www3.interscience.wiley.com doi : 10.1002/hyp.7640

Table V. Statistics of maximum infiltrated depth, I_{max}, maximum infiltration time, t_{max}, and their ratio, L, for the single ring infiltration tests

Variable	Average (-)	Standard deviation (-)	Minimum (-)	Maximum (-)	Median (-)	Coefficient of variation (-)	Sample size
I_{max} (mm)	86.6	18.1	11.5	114.4	90	0.21	58
t_{max} (min)	10.3	19.3	0.25	114.4	2.95	1.87	58
L (mm min^{-1})	55.9	79.6	0.36	340	26.7	1.42	58

Table VI. Statistics of sorptivity SR, S, saturated hydraulic conductivity, sorptivity MDI, hydraulic conductivity at -20mm for the three main land use classes where significant differences were identified: class KS1: broad leaved forest + small woods, class KS2: cultivated pasture + crop (bare soil after ploughing) + clearing, class KS3: permanent pasture + crop (wheat stubble) + coniferous forest + orchard. Std stands for standard deviation.

	Units	Number of samples SR (-)	S (mm s$^{-1/2}$)	K_s (mm s^{-1})	h_{VG} (mm)	Number of samples MDI (-)	$S(h$=-20mm) (mm s$^{-1/2}$)	$K_s(h$=-20mm) (mm s^{-1})	K_s/ $K_s(h$=-20mm) (-)
Class KS1	Average	10	5.22	1.39	-72.2	7	0.08	0.0031	448
	(Std)		(1.70)	(0.56)	(56.5)		(0.05)	(0.0027)	
	Median		4.64	1.20	-55.2		0.10	0.0021	571
	CV (%)		32.6	40.3	78.2		62.5	87.1	
Class KS2	Average	17	1.34	0.10	-74.0	12	0.11	0.0039	26
	(Std)		(0.67)	(0.11)	(60.3)		(0.05)	(0.0028)	
	Median		1.20	0.06	-65.5		0.10	0.0029	21
	CV (%)		50.0	110.0	81.5		45.4	71.8	
Class KS3	Average	30	2.95	0.44	-63.5	20	0.10	0.0075	59
	(Std)		(2.18)	(0.63)	(41.8)		(0.05)	(0.0067)	
	Median		2.47	0.24	-64.7		0.09	0.0049	49
	CV (%)		73.9	143.2	65.8		50.0	89.3	
All	Average	57	0.59	2.87	-68.1	37	0.10	0.0056	515
	(Std)		(0.12)	(2.18)	(49.8)		(0.052)	(0.0054)	
	Median		2.05	0.22	-64.8		0.10	0.0047	47
	CV (%)		20.3	76.0	73.1		52.0	96.7	

Author-produced version of the article published in Hydrological Processes, vol. 24, n° 17
The original publication is available at http://www3.interscience.wiley.com doi : 10.1002/hyp.7640

Table VII. Correspondence between the original detailed land use map of the Mercier catchment and the reclassified map according to the dry bulk (DB) and saturated hydraulic conductivity (KS) classes for mapping of porosity, saturated water content and saturated hydraulic conductivity.

Reclassified land use class	Original classes of the Mercier land use map	Porosity (-)	Saturated water content ($m^3\ m^{-3}$)	Near saturated hydraulic conductivity (-20 mm pressure) ($mm\ s^{-1}$)	Saturated hydraulic conductivity ($mm\ s^{-1}$)
DB1-KS1 (11)	Broad-leaved forest,	0.74	0.49	0.0031	1.39
DB1-KS3 (13)	Coniferous forest	0.74	0.49	0.0075	0.44
DB2-KS1 (21)	Scattered trees, hedges,	0.62	0.43	0.0031	1.39
DB2-KS2 (22)	Moors, heathland, fallow land,	0.62	0.43		
DB2-KS3 (23)	Pasture	0.62	0.43	0.0075	0.44
DB3-KS2 (32)	Ploughed fields, scattered grass,	0.48	0.34		
DB3-KS3 (33)	Orchards, berry plantation, wasteland, dump sites, spaces under construction, cemeteries	0.48	0.34	0.0075	0.44
Not sampled during the campaign	Impermeable surface (cement, asphalt), road networks, dirt roads, pervious artificial surfaces (gardens, trees)	Literature	Literature	Literature	Literature
Not relevant	Water bodies	NA	NA	NA	NA

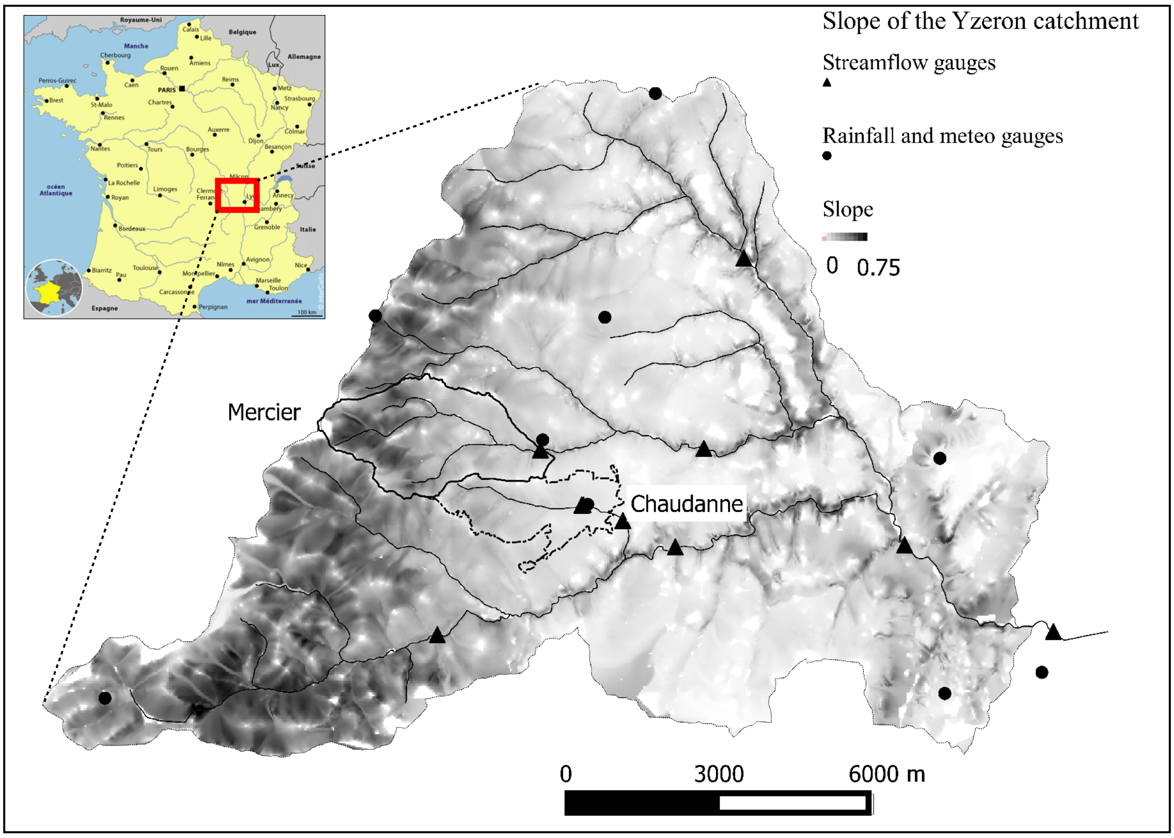

Figure 1: Location of the Yzeron catchment and of the two experimental sub-catchments (Mercier and Chaudanne). The grey scale shows the catchment slope with the highest values in dark and the lowest values in white. The symbols indicate the location of rainfall (points) and streamflow gauges (triangles).

Author-produced version of the article published in Hydrological Processes, vol. 24, n° 17
The original publication is available at http://www3.interscience.wiley.com doi : 10.1002/hyp.7640

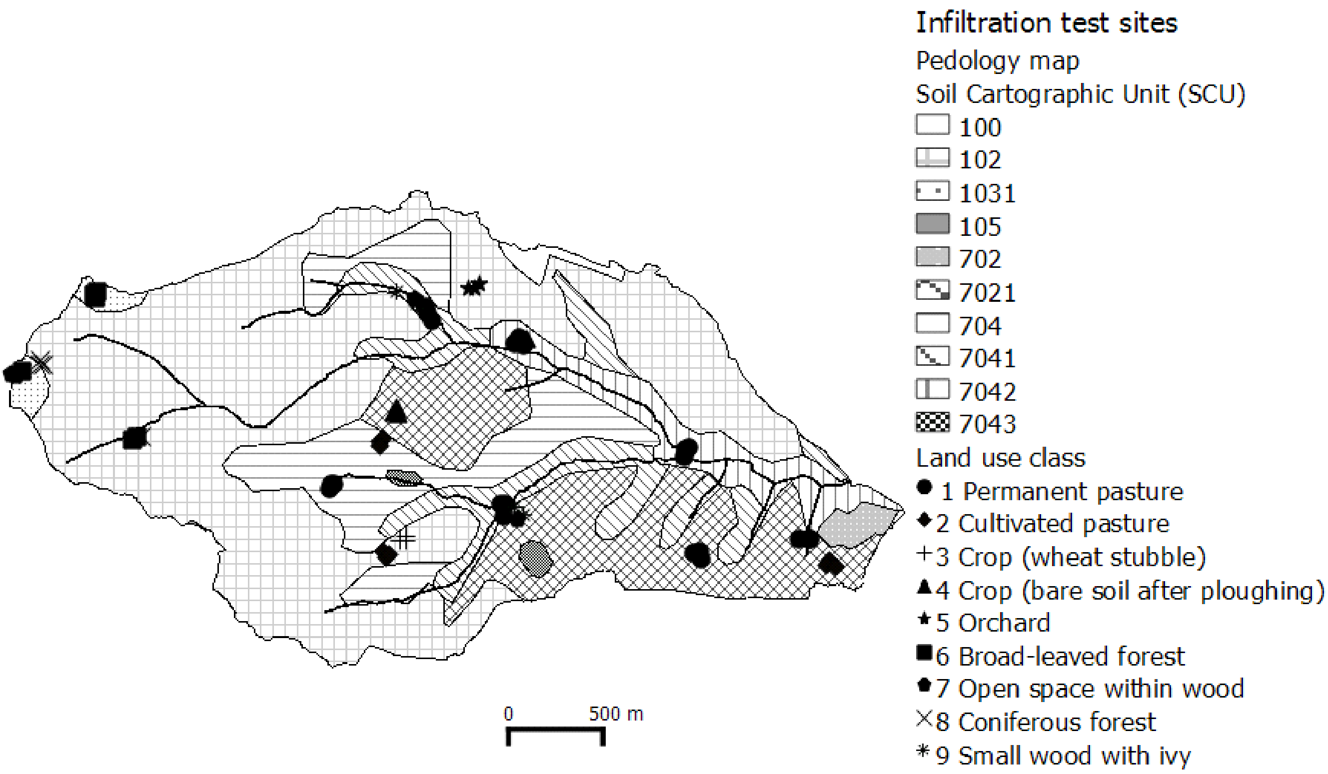

Figure 2: Pedology map of the Mercier catchment (from Sol Info Rhône Alpes http://www.rhone-alpes.chambagri.fr/sira/). The various colors correspond to the various Soil Cartographic Units defined in Table I. The symbols show the location of the infiltration test sites, with the various symbols corresponding to the various land use defined in Table I

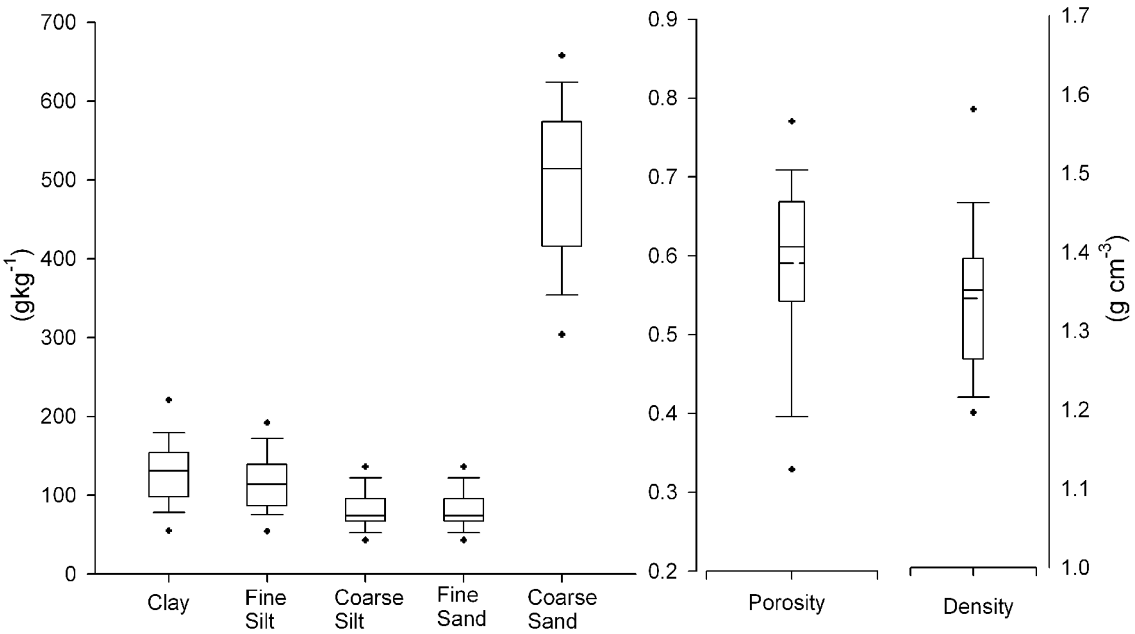

Figure 3: (a) Box plot of the fine particle size fractions and organic matter content (b) Box plot of the dry bulk density and porosity of the topsoil. On the box plots, boundaries indicates median, 25th and 75th quantiles, as vertical boxes error bars respectively: the top and bottom whiskers indicate the 10th and 90th percentiles and the points the minimum and maximum values.

Author-produced version of the article published in Hydrological Processes, vol. 24, n° 17
The original publication is available at http://www3.interscience.wiley.com doi : 10.1002/hyp.7640

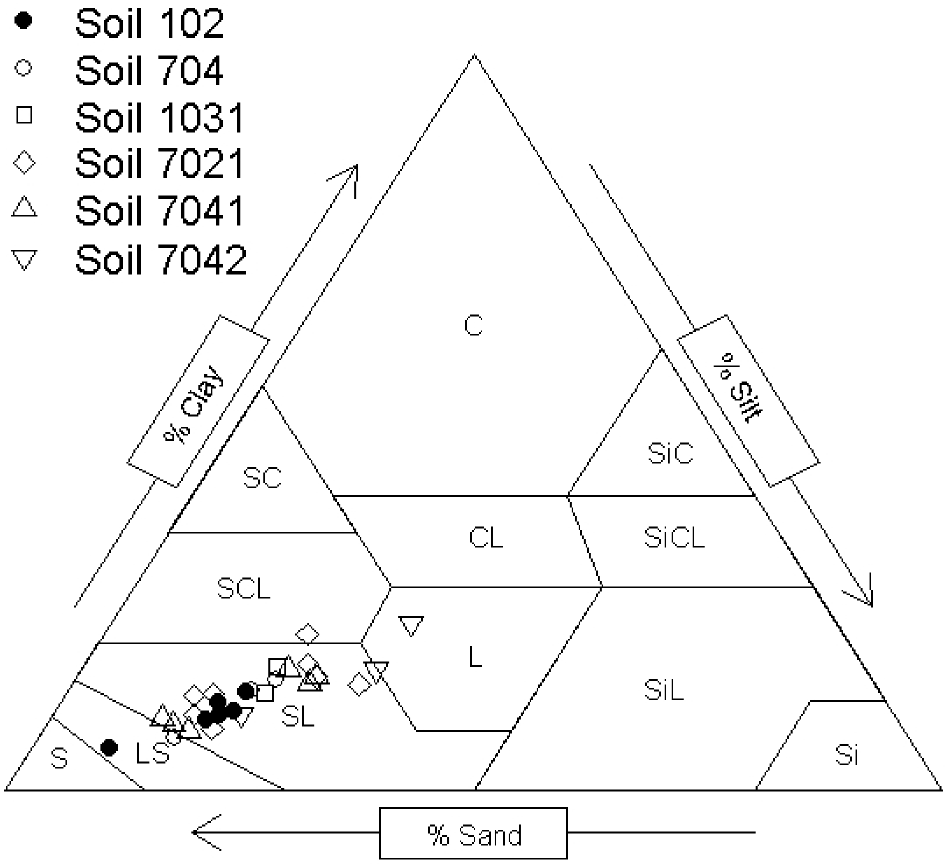

Figure 4: Presentation of the sampled points in the USDA textural triangle. The various symbols correspond to the different soil pedological units as defined in Table I..

Author-produced version of the article published in Hydrological Processes, vol. 24, n° 17
The original publication is available at http://www3.interscience.wiley.com doi : 10.1002/hyp.7640

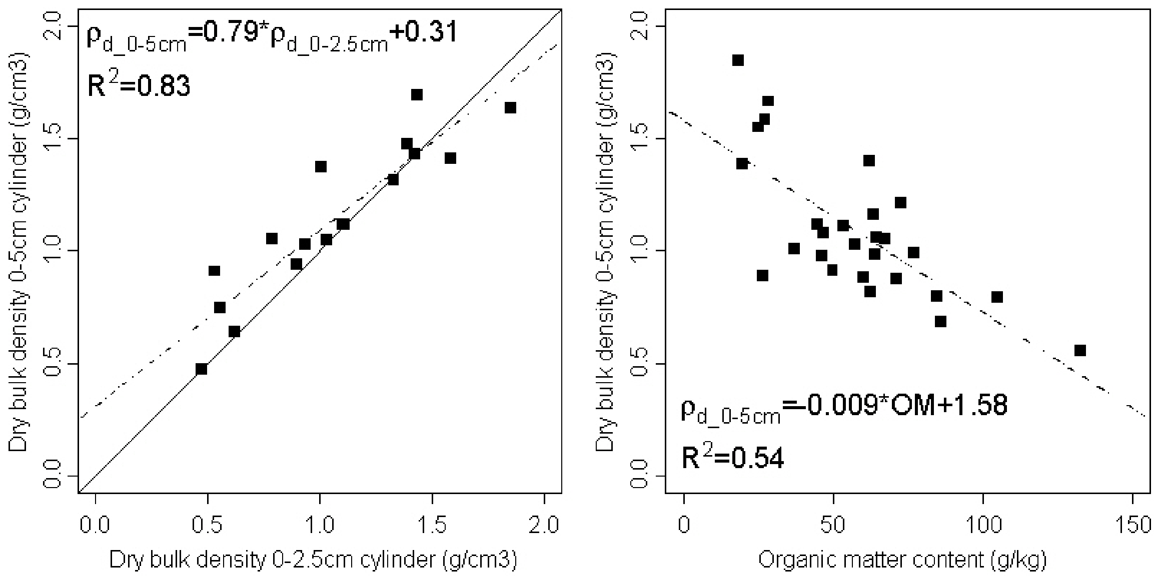

Figure 5: (a) Comparison of dry bulk density as measured using a 0-2.5 cm and 0-5 cm height cylinder. (b) Relationship between dry bulk density and organic matter content.

Author-produced version of the article published in Hydrological Processes, vol. 24, n° 17
The original publication is available at http://www3.interscience.wiley.com doi : 10.1002/hyp.7640

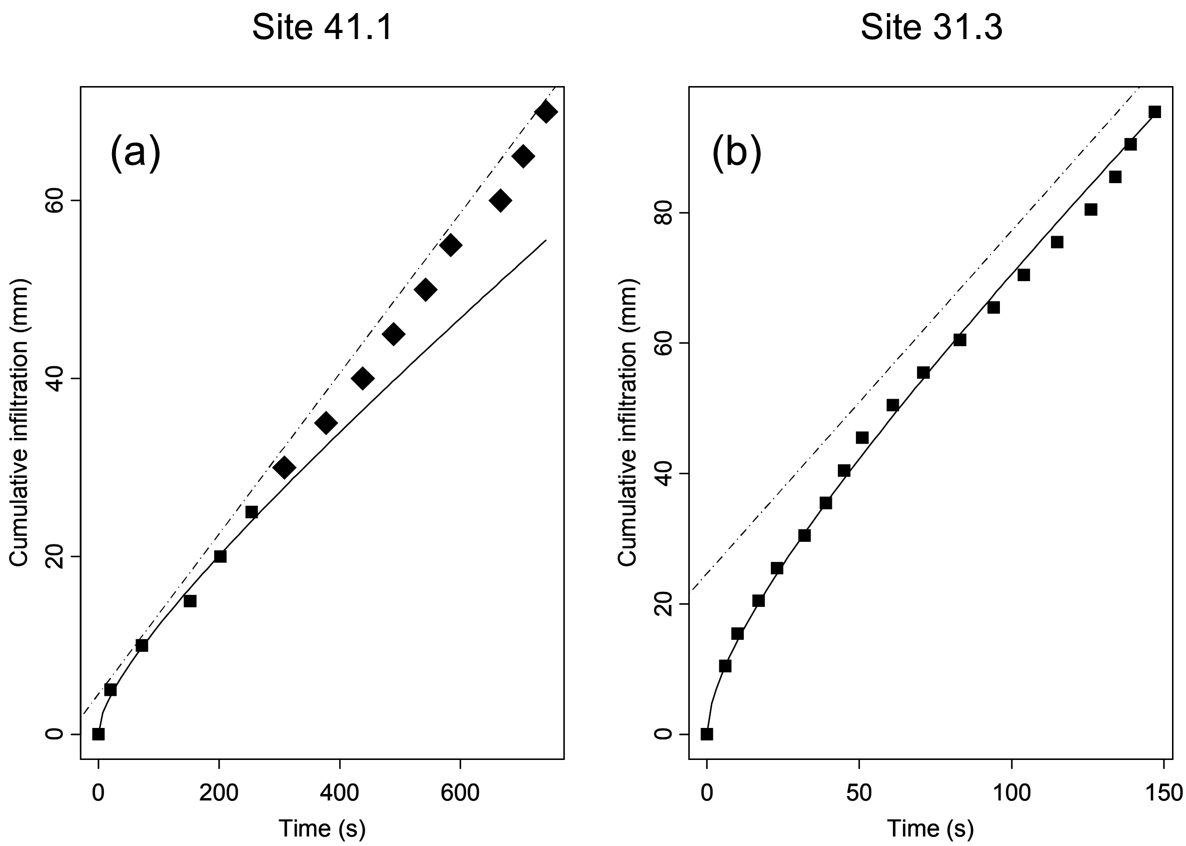

Figure 6. Observed (points) and fitted cumulative infiltration data for sites 41.1 (Open space in forest) and 31-3 (orchards). The full line is the fit of Eq. (6) for short time steps and the dashed line is the fit of Eq. (10) for large time steps. Eq. (6) was fitted to the points plotted with squares.

Author-produced version of the article published in Hydrological Processes, vol. 24, n° 17
The original publication is available at http://www3.interscience.wiley.com doi : 10.1002/hyp.7640

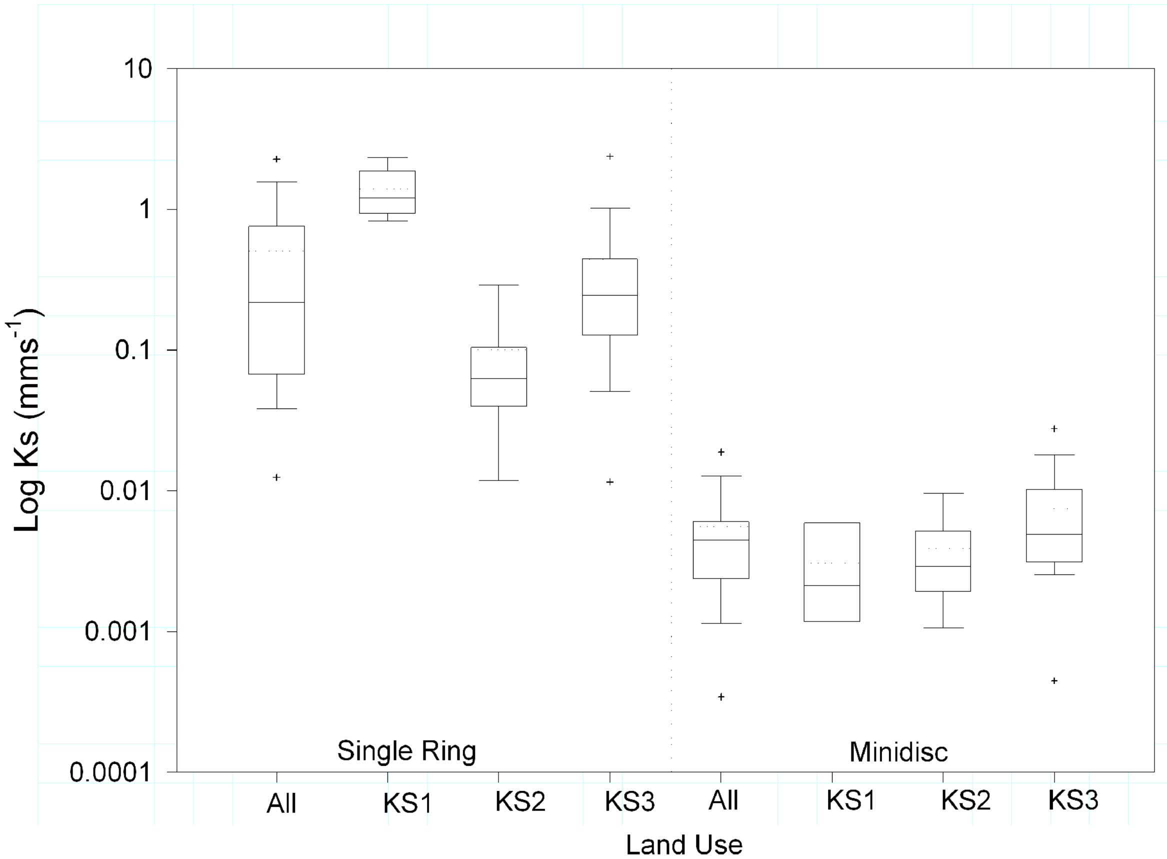

Figure 7. Box plots of saturated hydraulic conductivity (single ring) and hydraulic conductivity at -20 mm (mini-disk) for all the samples and the three identified classes KS1, KS2 and KS3.

Author-produced version of the article published in Hydrological Processes, vol. 24, n° 17
The original publication is available at http://www3.interscience.wiley.com doi : 10.1002/hyp.7640

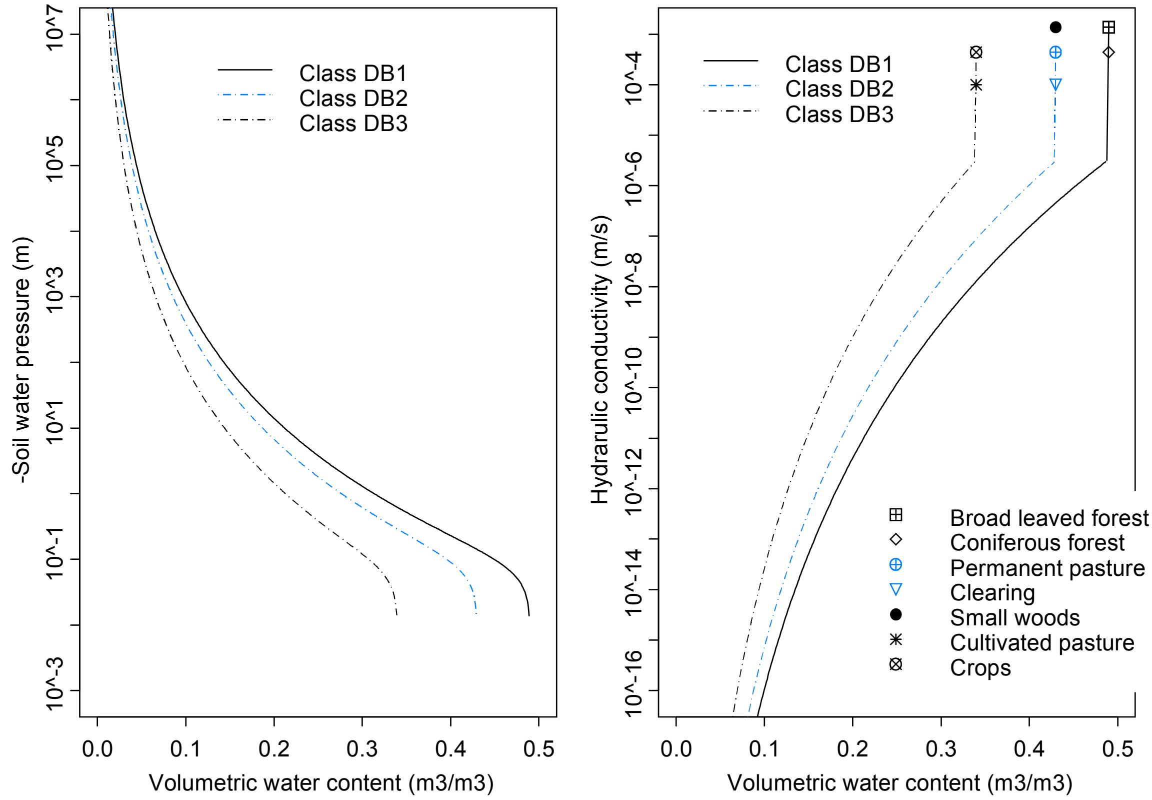

Figure 8. Estimated retention curves and hydraulic conductivity curves for the combination of classes DB1, DB2, DB3. Between near-saturated and saturated hydraulic conductivity, a linear relationship on the natural logarithm of hydraulic conductivity versus soil water content was assumed. The symbols are the saturated hydraulic conductivities for the various combinations of DB and KS classes: broad leaved forest (DB1-KS1); coniferous forest (DB1-KS3); permanent pasture (DB2-KS3); clearing (DB2-KS2); small woods (DB2-KS1); cultivated pasture (DB3-KS2); crops (DB3-KS3)..

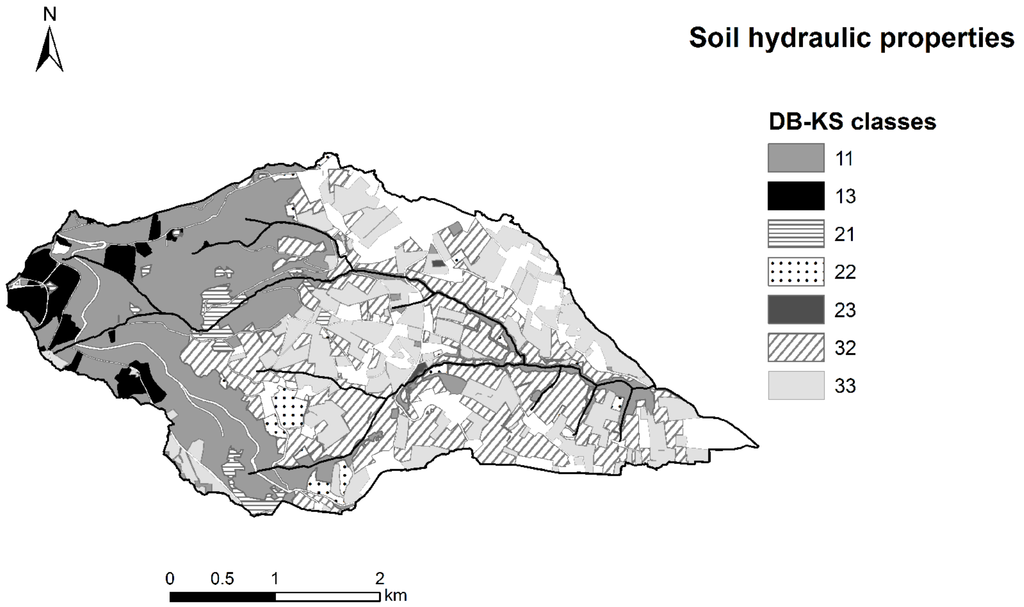

Figure 9. Mapping of soil hydraulic properties. The classes numbering is provided in Table VII. White surfaces correspond to the non sampled areas defined in Table VII.